Bull Mar Sci. 101(3):1191–1219. 2025
https://doi.org/10.5343/bms.2024.0021

Bulletin of Marine Science
research paper

The influence of mangrove forests on estuarine dynamics of dissolved organic matter

Mirco Wölfelschneider [1, 2 *]
Thorsten Dittmar [3, 4]
Vanessa Hatje [5]
Michael Seidel [3]

[1] *Leibniz Centre for Tropical Marine Research (ZMT), Bremen, Germany*

[2] *Faculty of Biology/Chemistry (FB2), Universität Bremen, Bremen, Germany*

[3] *Institute for Chemistry and Biology of the Marine Environment (ICBM), School of Mathematics and Science, Carl von Ossietzky Universität Oldenburg, Oldenburg, Germany*

[4] *Helmholtz Institute for Functional Marine Biodiversity at Carl von Ossietzky Universität*

Oldenburg (HIFMB), Oldenburg, Germany

[5] *Inst. de Química, Departamento de Química Analítica and Centro Interdisciplinar de Energia e Ambiente (CIEnAm), Universidade Federal da Bahia, Salvador, Brazil*

** Corresponding author email: <mirco.woelfelschneider@leibniz-zmt.de>*

ABSTRACT.—Mangroves play a critical role in shaping the composition of dissolved organic matter (DOM) in tropical estuarine systems. They act as bioreactors that transform and degrade imported organic matter before releasing it as DOM and export large amounts of leaf litter that leach additional DOM into estuarine waters. These processes are coupled with highly dynamic hydrological conditions in estuaries, creating complex systems that remain poorly understood. In this study, we used ultra-high resolution Fourier-transform ion cyclotron resonance mass spectrometry (FT-ICR-MS) to characterize the molecular composition of solid-phase extracted DOM along the Jaguaripe River estuary, Bahia, Brazil, and from mangrove leaf leachates in combination with environmental parameters. Our findings indicate that mangroves fringing the estuary are a significant source of dissolved organic carbon (DOC). DOM derived from mangroves was rich in sulfur-containing and saturated compounds with low oxygen-to-carbon (O/C) ratios, particularly during the dry season. Interestingly, during the rainy season, mangroves also appeared to act as a sink for total dissolved nitrogen (TDN) and aliphatic nitrogen-containing compounds. Mangrove leaf leachate DOM exhibited elevated levels of highly unsaturated compounds with low O/C ratios. We identified 432 unique compounds as indicators of DOM leached from mangrove leaf litter. Furthermore, we developed a novel molecular tracing index, I_{ManL}, which allowed us to successfully track mangrove leaf-derived DOM within the estuary and beyond. By combining our index with other established DOM indices, we gained a deeper understanding of how diverse DOM sources shape estuarine DOM pools, underscoring the significant influence of fringing mangroves in these systems.

Proceedings of the 6th Mangrove Macrobenthos and Management meeting

Guest Editors:
Juan Felipe Blanco-Libreros, Maria Fernanda Adame, Gustavo A Castellanos-Galindo, Samantha K Chapman, Karen Diele, José Ernesto Mancera Pineda, Kerrylee Rogers

Handling Editors:
Juan Felipe Blanco-Libreros, Rafael J Araújo

Date Submitted: 31 January, 2024.
Date Accepted: 11 November, 2024.
Available Online: 12 November, 2024.

Deltas and estuaries are important land-ocean interfaces shaping dissolved organic matter (DOM) and nutrient exchange between the two realms. Export processes at these interfaces often play significant roles in the budgets of essential elements, such as carbon and nitrogen, in the coastal waters (Medeiros et al. 2015a, Seidel et al. 2015a, Mori et al. 2019). DOM can generally be divided into autochthonous sources (formed by processes directly in the estuarine waters) and allochthonous sources (introduced from other systems, such as marine and terrestrial ecosystems, including mangrove forests). In tropical and subtropical regions, the coastlines of deltaic and estuarine areas with brackish waters are often dominated by dense mangrove forests (Spalding et al. 2010). These forests growing at the land-sea interface only occupy about 150,000 km^2 (Bunting et al. 2022), corresponding to less than 0.003% of the Earth's surface. Even so, estimates attribute more than 10% of recalcitrant DOM transported to the coastal oceans to mangroves (Dittmar et al. 2006). Nevertheless, how mangrove forests influence DOM and nutrient dynamics at the land-ocean interface is still not fully understood.

Mangroves are very heterogeneous ecosystems regarding physical-geochemical parameters (Bouillon et al. 2008). Ecosystems at the land-ocean interface are shaped by many environmental factors, in particular tidal dynamics (Medeiros et al. 2015b, Mori et al. 2019) and seasonal changes in precipitation (Medeiros et al. 2015b, Raymond et al. 2016). Especially seasonal changes not only directly influence nutrient and DOM dynamics in coastal tidal wetlands (e.g., Mori et al. 2019) but also indirectly by setting boundaries for biological processes and species dynamics (Mehlig 2001, Bernini and Rezende 2010, Hatje et al. 2021, Palit et al. 2022, Thomson et al. 2022). Previous studies have used conservative mixing models along salinity gradients to identify sinks and sources of nutrients and DOM (Seidel et al. 2015a, Mori et al. 2019). Furthermore, identified patterns of enrichment or depletion of nutrients and DOM were often coupled to seasonal changes such as precipitation (Dittmar et al. 2001, Dittmar and Lara 2001a, Seidel et al. 2017, Mori et al. 2019).

Another source of DOM in aquatic systems can be DOM released from plants and their leaf litter originating in terrestrial systems (Stenson et al. 2003, Brock et al. 2020, Hensgens et al. 2021). Studies investigating the persistence of DOM leached from leaves against degradation have shown that such DOM compounds are rapidly degraded by photo-oxidation and microbial degradation (Rossel et al. 2013, Hensgens et al. 2021). Thus, DOM freshly leached from terrestrial litter originating from inland systems is likely to be highly degraded by the time it reaches coastal waters. However, the proximity of mangroves to the coastal ocean probably means that less degraded organic compounds reach these waters. A potential pathway is through leaf litter leaching directly into coastal waters. Litter exports from different mangrove systems across the world have been estimated to be 383 (±315) g m^{-2} yr^{-1} (Golley et al. 1962, Lugo and Snedaker 1974, Boto and Bunt 1981, Woodroffe 1985a, Wattayakorn et al. 1990). Mangrove leaves leach up to 30% of their dry weight within the first 21 d in seawater (Camilleri and Ribi 1986, Tam et al. 1990, Chale 1993, Steinke et al. 1993, Davis and Childers 2007). This suggests a considerable potential for mangrove leaf litter to contribute significant amounts of DOM to estuarine and coastal waters. However, tracking such freshly released, and potentially readily degradable DOM remains challenging.

Ultra-high resolution Fourier-transform ion cyclotron resonance mass spectrometry (FT-ICR-MS) is a powerful tool for identifying compositional changes

in DOM within estuarine waters. Numerous studies have used this technique to gain insights into how the DOM composition evolves along estuaries and in wetlands (Rossel et al. 2013, Medeiros et al. 2015b, Hertkorn et al. 2016, Osterholz et al. 2016, Seidel et al. 2017). Tracing the sources of DOM in different aquatic ecosystems can be challenging but is crucial for a holistic understanding of biogeochemical drivers shaping DOM dynamics. However, DOM indices such as the one developed by Medeiros et al. (2016) for terrigenous DOM and the index by Knoke et al. (2024) for sulfurized porewater DOM highlight the effectiveness of such tools in unraveling the fate of DOM from different sources in complex environments.

In this study, we investigate the influence of various DOM sources on the estuarine DOM dynamics along a salinity gradient in a well-preserved mangrove-dominated estuary using FT-ICR-MS. We addressed the following research questions: How does the composition of DOM and concentration of dissolved nutrients change along an estuary with fringing mangroves? Can we track DOM leached from mangrove leaf litter using a novel molecular index (I_{ManL}) in estuarine waters? How do the contributions of DOM from mangrove leaf litter, the terrestrial hinterland, mangrove porewater, and coastal marine waters shape the DOM pools in the estuary? Lastly, we examined which DOM components are exported into estuarine waters and how their composition varies seasonally.

Material and Methods

Study Area.—The Jaguaripe River is located at the southern boundary of the Todos os Santos Bay, Bahia, Brazil (Fig. 1). It originates around 12°44′16.7″S and 39°24′07.8″W. Along its length of approximately 110 km, the Jaguaripe River drains about 2200 km^2, discharging its waters into the shelf region of the Atlantic Ocean (Hatje et al. 2010, Aguiar et al. 2019). The drainage area encompasses cultivated landscapes of open grassland, smaller urban areas, and mangrove forests. Mangrove forests, which dominate the margins of the Jaguaripe River estuary and cover around 4100 hectares, are considered relatively undisturbed by human activities (Hatje and Barros 2012, Hatje et al. 2021).

Sampling.—We sampled during the dry (13–21 February, 2019) and the rainy season (27 April–12 May, 2019). Over the last decade, the dry season lasted from August until February with an average rainfall of about 78 mm m^{-2} (INMET 2019). With an average precipitation of about 200 mm m^{-2}, the rainy season usually peaks in May and lasts 5 mo. Sample collections were conducted under the permit issued by the Instituto Chico Mendes de Conservação da Biodiversidade (ICMBio; SISBIO/61269-3).

Sampling campaigns during both seasons took place along five transects located in the lower half of the estuary (Fig. 1). Transects 1, 2, and 3 were characterized by mostly polyhaline conditions (salinity 18–30), whereas transects 4 and 5 were characterized by euhaline (salinity 30–40) conditions (Krull et al. 2014). Estuarine water was sampled <0.2 m below the surface using 5 L PET bottles which were rinsed three times with samples. During the sampling and the transport, samples were stored on ice in a cooling box. The five transects started approximately 15 km upstream from the river mouth and ended with the last transect crossing the river mouth. The transects were established 3 to 4 km apart from each other. The position of the second transect was

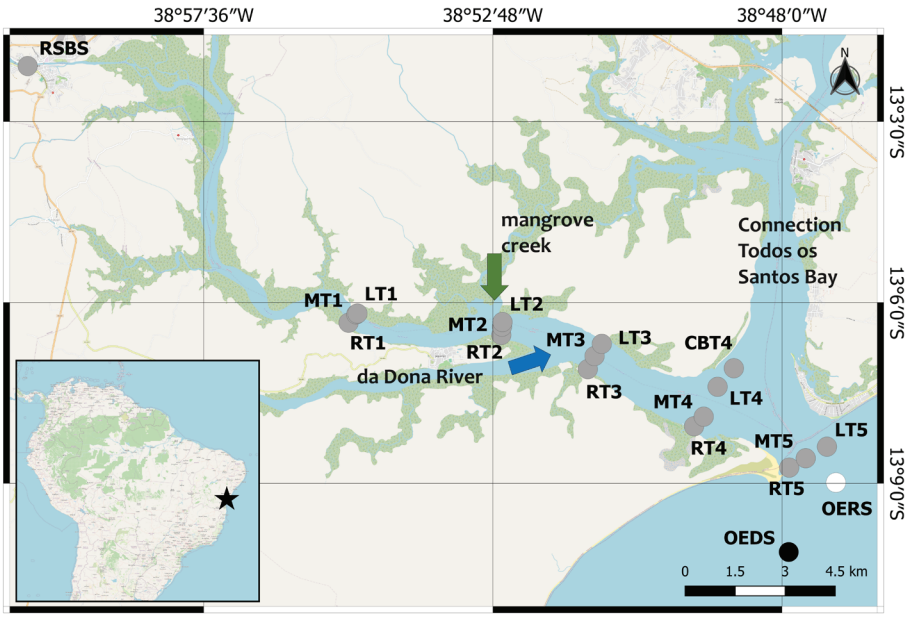

Figure 1. Map of the sampling area. Inset: overview map of South America with the location of the Jaguaripe River estuary (black star). Large map: sampling sites (grey circles) with the general locations of the five sampling transects and the upper river along the Jaguaripe River, Bahia, Brazil. RSBS = upper river, T1–T5 = transects 1–5, L = left position, M = middle position, R = right position, CB = connection Todos os Santos Bay. Sampling positions of the outer estuary in the dry season (black circle) and rainy season (white circle). Connections between the estuary and one of the largest tidal creeks (green arrow) and the merging with the da Dona River (blue arrow) are indicated. The green areas along the estuary represent mangrove forests. This map was created using the "Planet OSM" layer derived from OpenStreetMap.

next to the connection to a large mangrove creek. The third transect was located just after the confluence of the small da Dona River with the Jaguaripe River estuary. Each transect consisted of three sampling points. The two outer positions (LTX and RTX, with X being the number of the respective transect) were at the edges of the riverbanks during spring low tide at the left and right side of the estuary. The middle positions (MTX, with X being the number of the respective transect) were at the riverbed's deepest points of each transect. An exception was the fourth transect, which contained a fourth sampling position (CBT4) at the beginning of the channel connecting the estuary to the bordering Todos os Santos Bay in the north. The outer estuary was sampled as a coastal marine endmember (OEDS and OERS; Fig. 1). As a reference representing the DOM composition of the riverine endmember, we chose a location as far upriver as we could reach by boat. This point was located roughly 31 km upstream from the river mouth in the urban area of Nazaré, at which the river started to get much shallower and was covered with vast meadows of water grass (*Luziola spruceana*). At each sampling point, salinity, temperature, dissolved oxygen (DO; mg L^{-1}), and pH were measured using a multiparameter water probe (WTW, Multi 3430) with a pH (SenTix 980), oxygen (TetraCon 925), and conductivity sensor (SenTix ORP).

Leaf Leaching Experiment.—For the analysis of DOM compounds leached by mangrove leaves into the estuarine waters, we focused on the four mangrove species growing at the margins of the estuary. We did not include other terrestrial plant species, as in our working area, the Jaguaripe River estuary is almost exclusively fringed by extensive mangrove forest. The species present were, with decreasing abundance, *Rhizophora mangle*, *Avicennia schaueriana*, *Avicennia germinans* and *Laguncularia racemosa*. Senescent leaf samples of about 550 g (wet weight) were collected from >15 individual trees per mangrove species. All leaves were collected at the beginning of May 2019. To ensure a representative mixture of senescent sun and shadow leaves for our leaching experiment, we only collected leaves that could be plugged without exerting much force from all positions within the canopy. As *A. germinans* trees were relatively rare in the study area, we also had about 50% less wet weight of leaves for the leaching experiment compared to the other three mangrove species, even after adding additional leaves of earlier stages of senescence. After the collection, we immediately cleaned the surfaces of the leaves from sediment particles using tap water, weighed, and fully submerged them in 4 L of ultrapure water in one 5 L PET bottle per species. All bottles were newly acquired and precleaned with ultrapure water before adding the leaves. The incubation bottles had no headspace, creating an anoxic setup that minimized oxic microbial degradation of the released DOM. While some anoxic microbial fermentation may have occurred (Kusel and Drake 1996, Reith et al. 2002), microbial activity was likely limited as the senescent leaves were precleaned. The leaching process occurred over 3 d at ambient temperature (about 28 °C). The experiments were conducted with minimal UV exposure, due to the PET bottles acting as a barrier to UV light (Fechine et al. 2004, Oyane et al. 2014). However, this setup enabled us to partially simulate natural conditions. The anoxic environment was designed to preserve the bioavailable fraction of DOM by limiting microbial degradation. Additionally, limited photochemical degradation mimicked the breakdown of larger molecules, such as lignins, into smaller, more bioavailable compounds (Bauer and Bianchi 2011). This approach ensured that both DOM leaching and natural photochemical processes were captured.

Sample Preparation.—Water samples from transects and leaching experiment were filtered through a 1 µm Causa polypropylene depth cartridge filter and a 0.1 µm Causa polyethersulfone membrane cartridge filter using a peristaltic pump (MasterFlex L/S Cole Parmer). Filter cartridges, tubing, and filtration containers had been presoaked in acidified ultrapure water (pH 2, HCl) for 24 hr before usage and were rinsed with ultrapure water immediately before filtration. To ensure sample purity, over 2 L of initial flow-through were discarded. Following filtration, samples were acidified to pH 2 (HCl, p.a.) and were stored in dark at 4 °C until further processing. Process blanks were prepared before the first, after the 18th, and after the 36th filtrations and extractions using ultrapure water. For dissolved organic carbon (DOC) and total dissolved nitrogen (TDN) analyses, triplicate subsamples (each 30 ml) were taken. Styrene-divinyl benzene polymer-filled cartridges (Agilent Bond Elut PPL, 1 g) were used for the solid-phase extraction (SPE) of DOM (filtered, pH 2) as described by Dittmar et al. (2008). Extractions were run until the flow rate of the sample through the cartridge approached 0 resulting in extracted sample volumes between 1259 and 1429 ml. After extraction, the cartridges were desalted with ultrapure water (pH 2, HCl) and were dried with nitrogen, and then stored at

4 °C until transportation back to Germany. The cartridges were eluted in Germany with 6 ml methanol (LC grade) and extracts were stored at –20 °C before analysis.

DOC and TDN Analysis.—DOC and TDN concentrations from filtered and acidified subsamples and DOC concentrations from solid-phase extracts (SPE-DOC) were analyzed by high-temperature catalytic combustion with a Shimadzu TOC-VCPH instrument equipped with a TDN unit. For the SPE-DOC analysis, aliquots of the extracted SPE-DOM, ranging from 50 to 250 µl, were dried at 40 °C and subsequently re-dissolved in 10 ml acidified (pH 2) ultrapure water. Trueness and precision were tested against deep seawater reference material and low-carbon water (provided by DA Hansell, University of Miami, FL, USA), and both were better than 5%. The extraction efficiencies were calculated by dividing the SPE-DOC values by the DOC concentrations of the water samples taking into account the concentration factor of the SPE.

DOM Molecular Analysis.—We diluted the methanol extracts with HPLC grade methanol (Sigma Aldrich) and ultrapure water to DOC concentrations of 2.5 mg L^{-1} in a 1:1 (v/v) methanol to water mixture for FT-ICR-MS analysis. The solariX FT-ICR-MS (Bruker Daltonik GmbH, Bremen, Germany) used for the analysis was equipped with a 15 Tesla superconducting magnet (Bruker Biospin, Wissembourg, France). At a flow rate of 2 µL min^{-1}, the capillary voltage was set to 4 kV and the electrospray ionization in negative mode, the prediluted samples were infused into the electrospray source. For 0.1 s, the charged ions were accumulated in the hexapole before being transferred into the ICR cell. Data acquisition was performed in broadband mode using 8 megaword data sets and a scan range of 100–2000 Da. Two hundred scans were accumulated for each spectrum. All samples were analyzed in duplicates in a randomized order. To verify the instrument stability, before and after each block of 8 to 10 samples a laboratory-internal reference sample (SPE-DOM from North Equatorial Pacific Intermediate Water, *see* Green et al. 2014 for details) was measured. An internal calibration with a reference mass list of > 100 known $C_xH_yO_z$ molecular formulae covering the mass range targeted in the samples, achieved a mass accuracy of <0.1 ppm. Molecular formula attribution was done with ICBM-OCEAN (Merder et al. 2020). The method detection limit (MDL) was applied (Riedel and Dittmar 2014) with a minimum signal-to-noise ratio (S/MDL) of 3. The minimum signal to MDL ratio as backbone for recalibration was one using mean recalibration mode. Molecular formulae were assigned with a tolerance of 0.2 ppm as $C_{1–50}$, $H_{2–120}$, $O_{0–50}$, $N_{0–4}$, $S_{0–2}$, $P_{0–1}$, in the mass range of 100 to 1000 Da. Molecular formulae assignments were accepted if the molecular formula was present in >10% of the samples. Contaminants were identified and excluded manually by visual inspection of the spectra, and by referencing the SPE-DOM procedural blanks that were processed along with samples. Signal intensities of peaks of identified peaks were normalized to the sum of all peak intensities per sample. Molecular formulae containing isotopes (^{13}C, ^{18}O, ^{15}N, ^{34}S) were removed from the data table for further processing, and molecular formulae with molar ratios of oxygen to carbon (O/C) > 1, and hydrogen to carbon (H/C) > 2.5 were removed as well. Duplicate samples were averaged and then normalized, and molecular formulae were retained only when present in both duplicates.

For each sample, intensity weighted averages for formulae containing carbon (C), hydrogen (H), oxygen (O), nitrogen (N), sulfur (S), and phosphorus (P) atoms and double bound equivalents (DBE), molar ratios of hydrogen-to-carbon (H/C) and oxygen-to-carbon (O/C), as well as AI_{mod}, a parameter developed to identify aromatic and condensed aromatic structures in DOM molecular formulae data of ultra-high resolution MS (Koch and Dittmar 2006, 2016) were calculated as described by Seidel et al. (2014). We assigned seven DOM compound groups following Seidel et al. (2017) to the molecular formulae: (g1) polycyclic aromatics, (g2) highly aromatic compounds, which can include lignin degradation products, (g3) highly unsaturated compounds, (g4) unsaturated aliphatic compounds, (g5) saturated compounds with low O/C ratios, which can include lipids, (g6) saturated compounds with high O/C ratios, which can include carbohydrates, (g7) unsaturated aliphatic compounds containing N, which can include peptide degradation products. Such an assignment of compound groups has to be interpreted with caution, as the assigned molecular formula may consist of several different structural isomers (Zark et al. 2017). Nevertheless, it can be a valuable tool to identify biogeochemical drivers shaping DOM compositions in coastal systems (Osterholz et al. 2016, Seidel et al. 2017, Mori et al. 2019).

Index Calculations.—To identify the contribution of terrigenous DOM we followed the approach described by Medeiros et al. (2016). In short, the corresponding index referred to as I_{Terr} was calculated based on the normalized intensities of molecular formulae specified by Medeiros et al. [2016; sum magnitudes Terr/sum magnitudes (Terr + Mar)]. The 40 peaks identified in riverine sources associated with the highest positive $\delta^{13}C$ correlations were picked as the targeted terrigenous peaks (Terr) together with the 40 peaks with the highest negative correlations to $\delta^{13}C$ identified in ocean sources as the marine reference peaks (Mar) were used to calculate the index values for the samples as described by the authors.

The second index to evaluate the contribution of sulfidic porewater derived DOM (I_{SuP}) was calculated after Knoke et al. (2024). The index was initially developed for the purpose of tracking and identifying the contribution of DOM from sulfidic porewater originating in mangrove forest sediments. The index was calculated based on the normalized intensity of molecular formulae described in Knoke et al. [2024; sum magnitudes SuP/sum magnitudes (SuP + Mar)]. The 40 peaks identified in mangrove porewater samples are terrigenous molecular formulae containing S that are strongly correlated with Ba concentrations. They were picked as the targeted sulfurized, porewater-derived peaks (SuP) together with the 40 peaks identified by Medeiros et al. (2016) as the marine reference peaks (Mar). These peaks were used to calculate the index values for the samples as described by the authors.

To identify the contribution of DOM leached from mangrove leaves into coastal waters we developed a third molecular index. We selected molecular formulae of interest from all formulae identified unambiguously from mangrove DOM leaf leachates of any mangrove species sampled after subtraction of formulae identified in any of the endmember samples. This ensured the exclusion of molecular formulae from DOM of other primary producers, such as terrestrial plants located upstream or coastal phytoplankton. Our selections of endmembers were based on salinity values. Samples collected from location "RSBS" with salinities of 0 (rainy season) and 5.3 (dry season) represented the riverine and samples from location "LT5"

with salinities of 34.6 (rainy season) and 35.6 (dry season) represented the marine endmembers. Locations at the estuary mouth had equally high salinities in the dry season. To identify the sample with the highest impact of marine input and consequently the lowest impact of terrestrial input of the three locations we used the calculated I_{Terr} values of these samples. 622 molecular formulae were retained after subtracting all formulae identified in either of the endmember samples. Previous studies found high levels of highly unsaturated DOM compounds ($H/C < 1.5$, $AI_{mod} \leq 0.5$), especially with O/C ratios lower than 0.5 being leached from decaying leaf litter (Brock et al. 2020, Hensgens et al. 2021). Thus, we selected 40 molecular formulae of highly unsaturated compounds with low O/C ratios that were most abundant in the mangrove leaf leachates (ManL; Supplementary Table S1). These, together with the marine DOM molecular formulae identified by Medeiros et al. (2016; Mar), were used to calculate I_{ManL}, indicative of the direct input of DOM leached from mangrove leaves [sum magnitudes ManL/sum magnitudes (ManL + Mar) × 100].

Conservative Mixing Model.—To assess how concentrations of the measured DOC, TDN, and the abundance of the defined DOM compound groups deviated from a conservative two-end-member mixing with fluvial and marine endmembers, we applied linear regression analyses as described by Seidel et al. (2015a). The relative abundances of the DOM compound groups were scaled to the DOC concentrations of each corresponding sample before the normalization as described by Seidel et al. (2017). The calculated Δmix indicates the deviation of measured values and relative abundances of DOM compound groups from calculated conservative mixing. The selection of the riverine and marine endmembers was based on the lowest and highest salinity values respectively, as described earlier. To compensate for the potentially introduced bias of the DOC scaling for the compound groups, we decided to define possible differences as meaningful, if they differed from the conservative mixing behavior by at least 10% and by the mixing behavior seen in the normalized DOC values by at least two-fold. It is important to note that the Jaguaripe estuary is a complex system in which a simple linear mixing between two endmembers may not fully represent all source contributions. However, we intended to get a first-order insight into the dynamics of the DOM composition by this simplified approach. Deviations from the model can thus indicate an enrichment or depletion of DOM through interactions with the fringing mangroves, as well as the reworking of DOM compounds along the salinity gradient.

Statistical Analyses.—Multivariate statistical analyses were done using R v3.6.0 (R Core Team 2019) and the package vegan (Oksanen et al. 2020). For comparison of the DOM molecular composition of our samples, we performed a principal coordinate analysis (PCoA) on a Bray–Curtis dissimilarity matrix calculated from the normalized signal intensities of the assigned molecular formulae. Based on the eigenvalues of the PCoA axes, we calculated percentages of relative importance (Mori et al. 2019). Using the envfit function provided by the vegan package, we fitted explanatory environmental parameters and intensity-weighted averages of DOM compound groups to the PCoA scores. Correlations were tested based on 1000 permutations and considered significant if $P \leq 0.1$. Linear relationships between DOM molecular compositions and environmental parameters were determined by using Pearson correlation analyses, allowing us to identify significant gradients and thus potential environmental drivers.

Results

Biochemical and Physicochemical Parameters.—Water temperatures in the dry season ranged between 29.5 and 32.0 °C, decreasing downstream along the transects (Fig. 2A), with the 3rd transect exhibiting slightly higher temperatures. Water temperatures of the rainy season were between 25.9 and 28.9 °C, about 3 °C lower compared to the values of the dry season (Figs. 2B and 3B). Temperatures followed a similar trend as in the dry season decreasing downstream.

In the dry season, the lowest salinity (5.3) was at the upper river (RSBS; Fig. 2A). The highest salinity (35.6) was shared between the sampling positions MT5, LT5, and CBT4 (Fig. 2C). Except for the 5th transect, the middle position of each transect had lower salinity values compared to its flanking positions. Along transects, salinity slightly increased with decreasing distance to the coastal ocean, except transect 3, at which the salinity values were slightly lower compared to neighboring transects. Salinity levels of the rainy season ranged between 0 and 34.6 taken at locations of the upper river (RSBS) and the left sampling point of transect 5 (LT5) respectively (Fig. 3C). Downstream along the estuary, there was a trend of increasing salinity values from about 20 at the furthest upstream transect to about 34 at the furthest oceanward transect. The exception of this trend was the middle and left position of the 2nd transect (MT2 & LT2), which showed a drastic decrease in salinity to 11.2 and 9.8 respectively.

DO values ranged from 2.22 mg L^{-1} for the upper river location (RSBS) to 6.57 mg L^{-1} at the left position of the 5th transect (LT5). In the rainy season, DO values were between 4.30 mg L^{-1} for the position MT1 and 6.41 mg L^{-1} for the outer estuary location (OERS; Fig. 3D). Only for the rainy season, DO concentrations decreased with increasing distance from the coastal ocean (Fig. 3D).

In the dry season, pH values ranged from 7.26 at the upper river (RSBS) to 8.25 at LT4. In the rainy season, pH values were highest (8.14) at the outer estuary, and lowest (7.36) at the upper river (RSBS). The trends in both seasons of increasing values towards the coastal ocean were only interrupted for the rainy season by low pH values (7.27) at the second transect (MT2, LT2; Fig. 3E).

Highest DOC and TDN values of 706 and 137 μmol L^{-1}, respectively, were found in the upper river in the dry season (RSBS; Fig. 2F and G). The lowest DOC concentration of 106 μmol L^{-1} was found at position LT5, whereas the lowest level of TDN (8.68 μmol L^{-1}) was found at LT4. The outer estuary had values of 138 μmol L^{-1} for DOC and 18.61 μmol L^{-1} for TDN concentrations. DOC concentrations decreased with increasing salinity from the upper river to the coastal ocean (Fig. 2F). A pattern of decreasing TDN concentrations with increasing salinity was not observed (Fig. 2G). The highest DOC concentration was found during the rainy season at the riverine endmember (RSBS; 939 μmol L^{-1}; Fig. 3F). The lowest DOC concentration of 112 μmol L^{-1} was found at MT5 (5th transect). TDN concentrations were between 103 and 9 μmol L^{-1} between riverine and coastal ocean endmembers (RSBS and OERS) respectively (Fig. 3G). Overall, DOC and TDN concentrations decreased with increasing salinity from the upper river to the coastal ocean (Fig. 3F and G).

DOM Molecular Composition.—Molecular analysis of the 108 SPE-DOM samples via FT-ICR-MS yielded overall 8788 molecular formulae with molecular masses between 101 and 800 Da. Extraction efficiencies were 67% ± 12% (n = 96) on

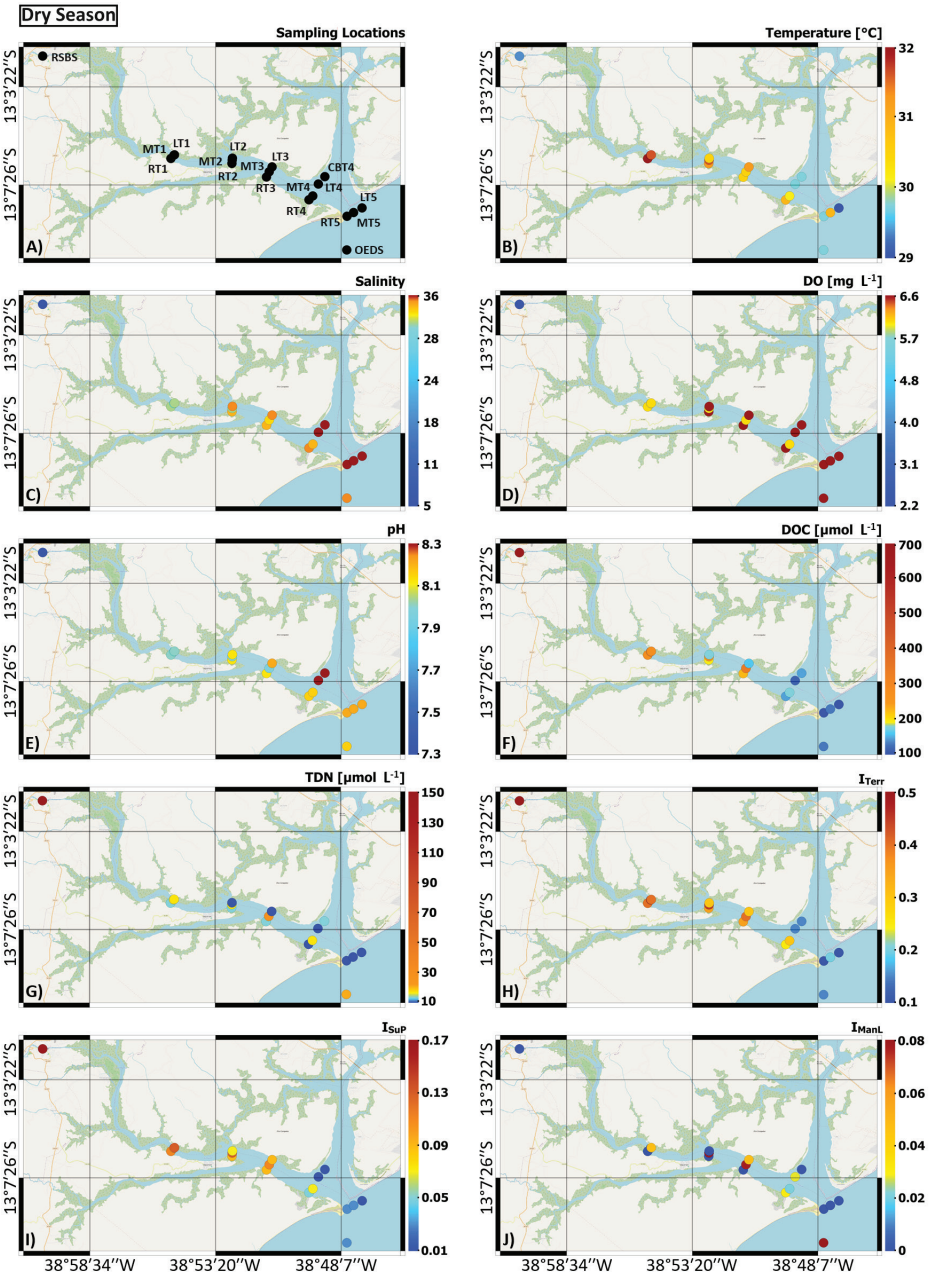

Figure 2. Surface water properties in the dry season and sampling locations along the Jaguaripe River estuary. (A) Sampling locations, (B) temperature (°C), (C) salinity, (D) dissolved oxygen (DO; mg L^{-1}), (E) pH, (F) dissolved organic carbon (DOC; µmol L^{-1}), (G) total dissolved nitrogen (TDN; µmol L^{-1}), (H) I_{Terr}, (I) I_{SuP}, and (J) I_{ManL}.

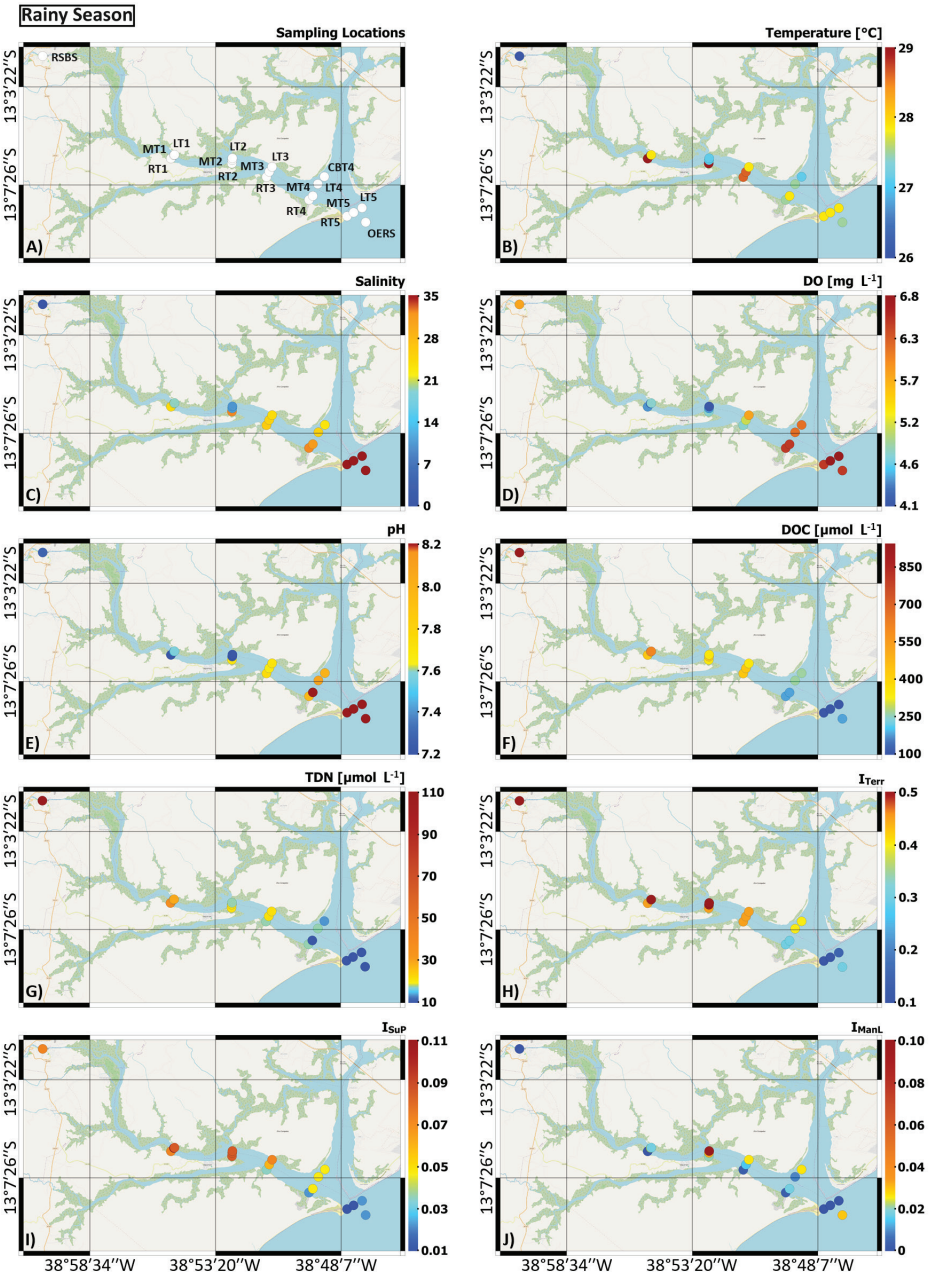

Figure 3. Surface water properties in the rainy season and sampling locations along the Jaguaripe River estuary. (A) Sampling locations, (B) temperature (°C), (C) salinity, (D) dissolved oxygen (DO; mg L^{-1}), (E) pH, (F) dissolved organic carbon (DOC; µmol L^{-1}), (G) total dissolved nitrogen (TDN; µmol L^{-1}), (H) I_{Terr}, (I) I_{SuP}, and (J) I_{ManL}.

Table 1. Characteristics of molecular formulae [intensity-weighted averages (intensity-weighted standard deviation)] of the five transects along the estuary of the Jaguaripe River in the dry season. Formulae = formulae present in respective samples, mass (Da) = intensity-weighted molecular mass in Dalton. Element contribution: C = carbon, H = hydrogen, O = oxygen, N = nitrogen, S = sulfur, P = phosphorous. Molar ratios: H/C = hydrogen to carbon ratio, O/C = oxygen to carbon ratio. Molecular indices: AImod as described by Seidel et al. (2014), DBE = double bound equivalents.

	Transect 1	Transect 2	Transect 3	Transect 4	Transect 5
Formulae	3,764 (727)	4,057 (689)	4,255 (793)	3,714 (718)	3,114 (184)
Mass (Da)	371 (8)	377 (3)	379 (10)	386 (4)	389 (7)
C	17.9 (0.2)	18.1 (0.1)	18.1 (0.2)	18.5 (0.1)	18.7 (0.2)
H	20.8 (0.2)	21.4 (0.4)	21.3 (0.2)	22.6 (0.8)	23.5 (0.5)
O	8.1 (0.3)	8.3 (0.1)	8.4 (0.4)	8.5 (0.2)	8.5 (0.3)
N	0.18 (0.02)	0.22 (0.01)	0.22 (0.03)	0.28 (0.05)	0.31 (0.03)
S	0.11 (0.01)	0.09 (0.02)	0.10 (0.01)	0.06 (0.03)	0.04 (0.01)
P	0.0003 (0.0005)	0.0005 (0.0004)	0.0004 (0.0006)	0.0019 (0.0022)	0.0030 (0.0018)
H/C	1.16 (0.02)	1.17 (0.02)	1.17 (0.02)	1.21 (0.04)	1.25 (0.02)
O/C	0.45 (0.01)	0.46 (0.01)	0.46 (0.01)	0.46 (0.01)	0.45 (0.01)
AI_{mod}	0.32 (0)	0.31 (0.01)	0.31 (0.01)	0.28 (0.03)	0.26 (0.01)
DBE	8.57 (0.25)	8.52 (0.20)	8.58 (0.28)	8.39 (0.36)	8.14 (0.10)

a carbon basis and extraction efficiency was uncorrelated to salinity, demonstrating no preferential extractions of marine over terrestrial DOM or vice versa. The mean number of C, H, N, and P atoms in molecular formulae as well as intensity-weighted average H/C ratios, and AI_{mod} values were lower for the upstream transects compared to transect closer to the coastal ocean (Table 1). Averaged numbers of S atoms in molecular formulae, mean values of DBE, and mean molecular masses decreased from mangrove fringed transects upriver towards transect without fringing mangroves closer to the river mouth. The number of O atoms present and the O/C ratios were very similar across all transects.

In the rainy season, the number of molecular formulae decreased on average for samples from upriver transects compared to samples taken near the coastal ocean (Table 2). Averaged numbers of S atoms in molecular formulae and intensity-weighted average AI_{mod} decreased from the upper river transects towards the coastal ocean transects, while intensity-weighted average H/C ratios increased. Averaged numbers

Table 2. Characteristics of molecular formulae [intensity-weighted averages (intensity-weighted standard deviation)] of the five transects along the estuary of the Jaguaripe River in the rainy season. Formulae = formulae present in respective samples, mass (Da) = intensity-weighted molecular mass in Dalton. Element contribution: C = carbon, H = hydrogen, O = oxygen, N = nitrogen, S = sulfur, P = phosphorous. Molar ratios: H/C = hydrogen to carbon ratio, O/C = oxygen to carbon ratio. Molecular indices: AImod as described by Seidel et al. (2014), DBE = double bound equivalents.

	Transect 1	Transect 2	Transect 3	Transect 4	Transect 5
Formulae	3,915 (861)	4,441 (270)	3,489 (442)	3,391 (534)	2,775 (391)
Mass (Da)	373 (11)	391 (9)	392 (3)	379 (7)	384 (4)
C	18.3 (0.3)	19.0 (0.4)	19.0 (0.1)	18.6 (0.2)	18.6 (0.1)
H	20.8 (0.3)	20.8 (0.1)	20.8 (0.2)	21.4 (0.2)	23.3 (0.1)
O	8.1 (0.4)	8.7 (0.3)	8.8 (0.2)	8.3 (0.3)	8.3 (0.2)
N	0.15 (0.03)	0.12 (0.04)	0.10 (0.02)	0.17 (0.03)	0.29 (0.03)
S	0.06 (0.01)	0.06 (0.01)	0.04 (0.01)	0.04 (0.01)	0.02 (0.00)
P	0.0011 (0.0014)	0.0003 (0.0001)	0.0001 (0.0001)	0.0011 (0.0006)	0.0038 (0.0010)
H/C	1.13 (0.03)	1.09 (0.03)	1.08 (0.01)	1.14 (0.01)	1.25 (0.01)
O/C	0.44 (0.02)	0.46 (0.01)	0.46 (0.01)	0.45 (0.01)	0.45 (0.01)
AI_{mod}	0.34 (0.01)	0.36 (0.02)	0.36 (0.01)	0.33 (0.01)	0.26 (0.01)
DBE	8.95 (0.44)	9.60 (0.43)	9.69 (0.19)	8.93 (0.19)	8.10 (0.13)

of H, P, and N atoms assigned to the identified compounds appeared comparable for transects 1 to 4, while averaged values for the 5th transect were much higher in comparison. Intensity-weighted averages of molecular masses were similar across all transects.

In the dry season, the PCoA analysis based on the dissimilarity matrix showed a clear separation of samples along different transects (Fig. 4A). Principal coordinate 1 (PC1), which explained 60% of the variability in DOM molecular composition, revealed a gradual progression of transects along the estuary. Transects closer to the coastal ocean (4 and 5) were positively correlated with environmental factors such as pH, salinity, and DO, as well as compound groups 3, 4, 6, and 7. High levels of highly unsaturated compounds and N-containing unsaturated aliphatics (groups 3 and 7) were strongly associated with the separation of samples along PC1. Unsaturated aliphatics without N and oxygen-rich saturated compounds (groups 4 and 6) were also correlated with PC1 but to a lesser extent. Samples closer to the river mouth were linked to N- and P-containing compounds. In contrast, samples from upstream transects and the riverine endmember correlated with higher DOC and TDN concentrations, S-containing compounds, and compound groups g1 and g2, as well as the indices I_{SuP} and I_{Terr}. Saturated compounds with low O/C ratios (group 5) were less strongly associated with samples further from the coastal ocean. Along principal coordinate 2 (PC2), the separation of samples was less distinct, but samples nearer to the coastal ocean were generally correlated with higher molecular masses and higher O/C values.

In the rainy season, PCoA showed a less distinct separation of samples across transects compared to the dry season (Fig. 4B). However, along PC1 (explaining 62% of variability), samples near the river mouth were generally on the positive side, while upriver samples were on the negative side, with two exceptions: an outer estuary sample and one from transect 2. Salinity, DO, pH, and compound groups 3, 4, 6, and 7 were positively correlated with samples near the river mouth, though the separation was less clear than in the dry season and shifted towards PC2. Samples on the negative side of PC1 were associated with higher DOC concentrations, S-containing compounds, and compound groups 1 and 2. Five samples from transects 2 and 3 showed stronger correlations with highly aromatic and polycyclic aromatic compounds, disrupting the pattern. These differences caused separation along PC2 (explaining 15% of variability), with the outer estuary sample strongly correlated with compound group 1.

SPE-DOM samples of the mangrove leaf leachates contained 432 unique molecular formulae not present in the riverine or marine endmember samples. Overall, the mangrove leaf leachates had increased intensity-weighted averages of S-contents (0.11 ± 0.02) and decreased levels intensity-weighted averages of N-contents (0.04 ± 0.03) compared to the marine and riverine DOM endmembers (Supplementary Table S2). The intensity-weighted average H/C ratios (1.16 ± 0.16), intensity-weighted average AI_{mod} (0.34 ± 0.09) and DBE values (9.39 ± 0.97) were between values from riverine and marine endmember samples. The marine endmembers were characterized by the highest level of intensity-weighted average H/C ratio (1.23) and the lowest levels of intensity-weighted average AI_{mod} (0.27) and DBE (8.35) and had a total of 542 compounds with unique formulae. The riverine endmember DOM had the lowest intensity-weighted average H/C ratio (1.11) and the highest levels for intensity-weighted average AI_{mod} (0.35), DBE (9.29), and levels of S-containing compounds

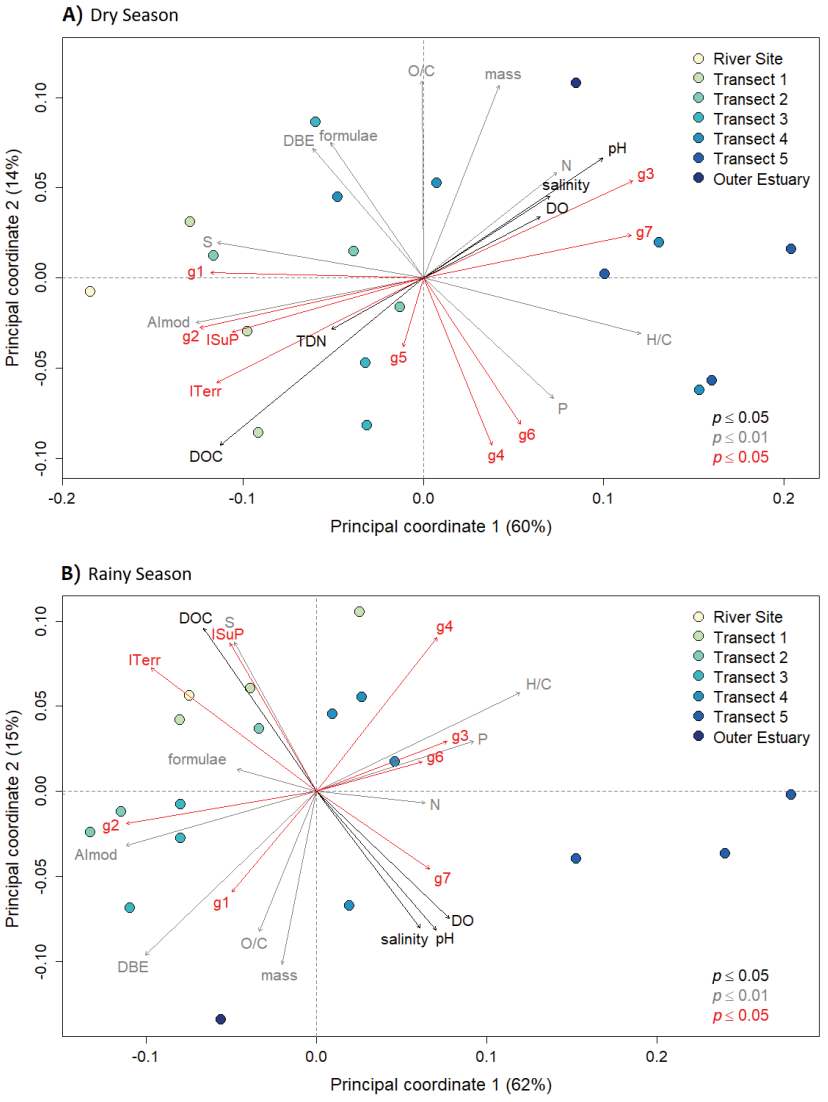

Figure 4. Principal coordinate analyses (PCoA) based on Bray–Curtis dissimilarity of the relative FT-ICR-MS signal intensities of DOM molecular formulae of surface water samples taken (A) in the dry season and (B) in the rainy season. Colored circles represent the different sampling locations: riverine endmember (yellow circles), transect 1 (orange circles), transect 2 (red circles), transect 3 (brown circles), transect 4 (purple circles), transect 5 (dark blue circles), and marine endmember (blue circles). Environmental parameters including DOC and TDN concentrations (black arrows) were significantly correlated with $P \leq 0.05$; intensity-weighted averages of DOM molecular parameters (grey arrows) were significantly correlated with $P \leq 0.01$, with N = nitrogen-containing compounds, S = sulfur containing compounds, P = phosphorous-containing compounds; intensity-weighted averages of DOM molecular compound groups after Seidel et al. (2017) and tracing indices after Medeiros et al. (2016) and Knoke et al. (2024; red arrows) were significantly correlated with $P \leq 0.05$, with g1 = polycyclic aromatics, g2 = highly aromatic, g3 = highly unsaturated compounds, g4 = unsaturated aliphatics, g5 = saturated compounds with low O/C ratios, g6 = saturated compounds with high O/C ratios, g7 = aliphatics containing N, I_{SuP} = index to identify the contribution of mangrove porewater DOM, I_{Terr} = index to identify the contribution of terrestrial DOM.

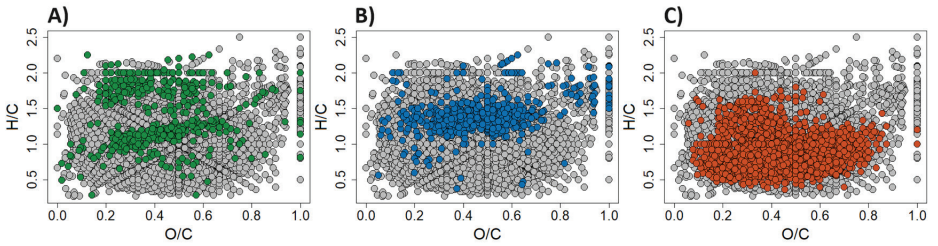

Figure 5. Van–Krevelen plots of DOM molecular formulae for (A) mangrove leaf leachates, (B) marine endmembers of both seasons, and (C) riverine endmembers of both seasons. Unique formulae for the three groups are colored (green = mangrove leaf leachates, blue = marine endmember, orange = riverine endmember). Shared formulae of all groups are colored in gray.

(0.08). In total, we identified 1637 unique compound formulae shared with neither the marine endmember nor the mangrove leaf leachates. A major cluster of unique molecular formulae from the mangrove leaf leachates was found in van–Krevelen space between intensity-weighted average H/C 1 and 1.2 (Fig. 5), alongside with a smaller cluster with H/C ratios of 1.5–2.0 and O/C ratios of 0.2–0.4. Unique marine endmembers molecular formulae were found with intensity-weighted average H/C ratios of 1.2–1.5 and O/C ratios of 0.3–0.7. Unique riverine molecular formulae were in the range of H/C ratios between 0.5 and 1.0 and between 0.4 and 0.7 for the intensity-weighted average O/C ratios. The riverine cluster overlapped partly with the mangrove leaf leachates and the marine endmember cluster. This overlap was mainly in the range of intensity-weighted average H/C ratios between 1.0 and 1.5 and O/C ratios of 0.2–0.4.

Endmember Mixing.—In the dry season, DOC-scaled relative abundances of compounds containing P heteroatoms, saturated compounds with high O/C ratios (group 6), and unsaturated aliphatics containing N (group 7) were lowest at the riverine endmember and increased closer to the coastal ocean (Fig. 6). The values of compound groups 6 and 7 show a large scatter around the model of conservative mixing. Compounds containing P heteroatoms were distinctly lower compared to the conservative mixing values. DOC and TDN concentrations, as well as DOC-scaled relative abundances of N and S-containing compounds, aromatic (group 1), highly aromatic (group 2), highly unsaturated (group 3), unsaturated aliphatic compounds (group 4), and saturated compounds with low O/C ratios (group 5) displayed opposing trends with the highest values of the river endmember and distinctly lower values at the marine endmember.

In the rainy season, DOC concentrations, S, and P containing compounds, and unsaturated compounds with low O/C ratios (group 5) had levels exceeding those expected from conservative mixing. These values differed distinctly from the mean deviation of the normalized DOC values to the conservative mixing. Concentrations of TDN and N-containing compounds were below conservative mixing values. The compounds of groups 1 to 4 displayed values higher compared to the conservative mixing, but these values were indistinguishable from those of the normalized DOC values. Saturated compounds with high O/C ratios (group 6) were undetectable in over half the samples, but values above 0 were mostly found in transects near the coastal ocean.

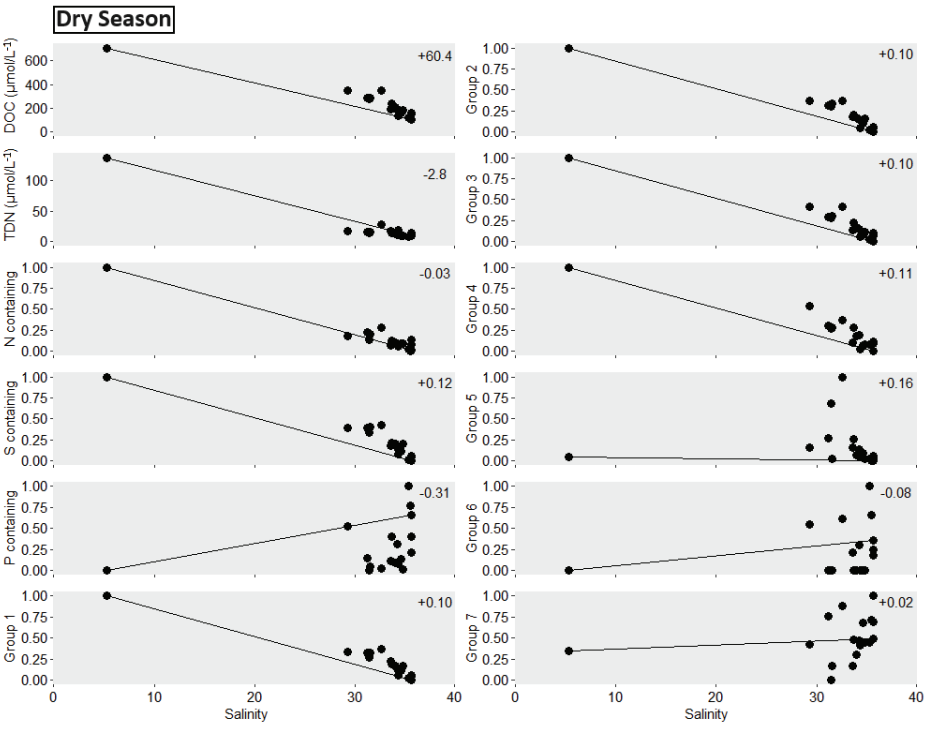

Figure 6. Conservative mixing plots of biochemical parameters and molecular DOM surface water parameters in the dry season. The theoretical conservative mixing behavior is represented by the solid black lines. For the abundance of biochemical parameters: concentrations of DOC (µmol L^{-1}) and TDN (µmol L^{-1}). For their minimum and maximum normalized and DOC scaled abundances of DOM molecular parameters and compound groups: N = nitrogen, S = sulfur, P = phosphorous containing DOM, g1 = polycyclic aromatics, g2 = highly aromatic, g3 = highly unsaturated compounds, g4 = unsaturated aliphatics, g5 = saturated compounds with low O/C ratios, g6 = saturated compounds with high O/C ratios, and g7 = aliphatics containing N. In-box numbers indicate whether is δmix is positive (+) or negative (−) for the respective parameter.

In the rainy season, relative abundances scaled to DOC concentrations of compounds containing P, saturated compounds with low O/C ratios (group 5), and unsaturated aliphatics containing N (group 7) increased from the riverine to the marine endmember (Fig. 7). Values of P-containing compounds and compounds from group 5 were above values expected from conservative mixing. Values for compounds from group 7 were below conservative mixing values. DOC and TDN concentrations, as well as DOC-scaled relative abundances of N- and S-containing compounds, aromatic (group 1), highly aromatic (group 2), highly unsaturated (group 3), and unsaturated aliphatic compounds (group 4) had values decreasing from the riverine to the marine endmembers. DOC concentrations and DOC-normalized values of the compound groups 2 to 4 were not distinctly higher compared to values expected from conservative mixing. For TDN concentrations, S-containing compounds and aliphatics containing nitrogen (group 7) values were distinctly lower than expected for conservative mixing. Values of DOC-scaled relative abundances of polycyclic aromatics and saturated compounds with low oxygen values (groups 1 and 5) were distinctly higher compared to values from conservative mixing. DOC-scaled relative abundances of saturated compounds with high O/C ratios (group 6) were

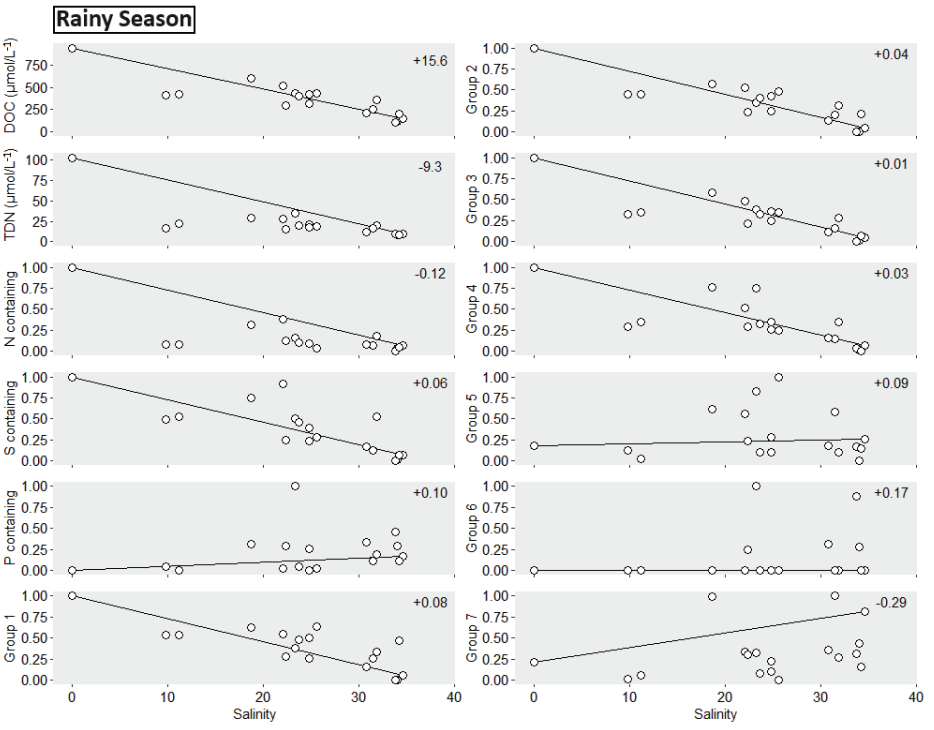

Figure 7. Conservative mixing plots of biochemical and molecular DOM surface water parameters in the rainy season. The theoretical conservative mixing behavior is represented by the solid black lines. For the abundance of biochemical parameters: concentrations of DOC (µmol L^{-1}) and TDN (µmol L^{-1}). For their minimum and maximum normalized and DOC scaled abundances of DOM molecular parameters and compound groups: N = nitrogen, S = sulfur, P = phosphorous containing DOM, g1 = polycyclic aromatics, g2 = highly aromatic, g3 = highly unsaturated compounds, g4 = unsaturated aliphatics, g5 = saturated compounds with low O/C ratios, g6 = saturated compounds with high O/C ratios, and g7 = aliphatics containing N. In-box numbers indicate whether δmix is positive (+) or negative (−) for the respective parameter.

mostly close to zero but had values above conservative mixing in transects closer to the marine endmember.

Tracing OM Sources.—In the dry season, I_{Terr} values ranged from 0.096 (LT5) to 0.471 (RSBS), decreasing toward the coastal ocean, with middle transect locations generally showing higher values (Table 3, Fig. 2H). Left-side locations of transects 2–5 had lower I_{Terr} values than their right counterparts, except for a slight reversal upriver (Fig. 2H). I_{SuP} values were between 0.014 and 0.168, following a similar pattern as I_{Terr}, peaking at the middle positions (Fig. 2I), while I_{ManL} values (0 to 0.081) had no clear spatial pattern (Fig. 2J).

In the rainy season, I_{Terr} values were highest at LT2 (0.510) and RSBS (0.500) and lowest at RT5 (0.160), decreasing toward the coastal ocean, with left-side positions consistently showing higher values (Table 4, Fig. 3H). I_{SuP} values ranged from 0.006 to 0.112, peaking at MT1, decreasing seaward (Fig. 3I). I_{ManL} values were highest at LT2 (0.104), with a general pattern of decreasing values from left to right along transects 2 to 4, while transect 1 showed the highest value at its middle position (Fig. 3J).

Table 3. Index values calculated for the samples along the estuary of the Jaguaripe River in the dry season.

Sampling locations	I_{Terr}	I_{SuP}	I_{ManL}
RSBS	0.470	0.168	0
RT1	0.383	0.104	0
MT1	0.407	0.113	0
LT1	0.385	0.132	0.005
RT2	0.305	0.083	0
MT2	0.394	0.126	0.008
LT2	0.294	0.072	0
RT3	0.329	0.083	0
MT3	0.379	0.116	0.008
LT3	0.284	0.090	0.005
RT4	0.248	0.064	0.003
MT4	0.296	0.077	0.002
LT4	0.154	0.026	0.003
CBT4	0.156	0.027	0
RT5	0.135	0.031	0
MT5	0.181	0.037	0
LT5	0.096	0.014	0
OEDS	0.156	0.040	0.008

Discussion

Seasonal Variability and Nonconservative Behavior of DOC and TDN Concentrations.—Environmental parameters deviated from conservative mixing along the estuary, with elevated DOC concentrations indicating an additional source in the mangrove-fringed section, particularly during the dry season (Figs. 6 and 7). DOC enrichments were more pronounced in the dry season, as indicated by higher positive deviations from conservative mixing compared to the rainy season (compare Δmix values in Figs. 6 and 7). Tidal-driven porewater outwelling from the mangroves was likely responsible for this additional DOC input in the estuary (Dittmar et al. 2006, Kristensen et al. 2008, Maher et al. 2013, Ray et al. 2018), especially during the dry season (Dittmar and Lara 2001b, Santos et al. 2009, Mori et al. 2019). In the rainy season, however, this input was not evident. Additionally, the observed DOC concentrations were much higher in the rainy season compared to the dry season. In the rainy season, DOC concentrations were generally higher in the sampling transects than in the dry season, which was likely due to increased terrestrial runoff, which may also mask the input of DOC by tidal pumping (Raymond et al. 2016, Seidel et al. 2017, Letourneau and Medeiros 2019, Mori et al. 2019).

TDN concentrations in the dry season closely matched with conservative mixing values, suggesting no significant nitrogen input or removal within the mangroves (Fig. 6). However, during the rainy season, TDN concentrations were notably lower than values calculated by conservative mixing, indicating a seasonal sink of dissolved nitrogen along the estuary (Fig. 7). Dynamics of dissolved nitrogen in mangrove-dominated estuaries are characterized by complex biogeochemical factors, such as microbial activity and uptake by coastal vegetation (Reis et al. 2017, Mori et al. 2019). Whether a mangrove forest acts as a source or a sink of N strongly depends on its utilization capacity. Thus, mangrove forests can only act as nitrogen sources, if the nitrogen availability in the forest exceeds the demand of the mangroves and its

Table 4. Index values calculated for the samples along the estuary of the Jaguaripe River in the dry season.

Sampling locations	I_{Terr}	I_{SuP}	I_{ManL}
RSBS	0.500	0.076	0
RT1	0.452	0.071	0
MT1	0.467	0.112	0.025
LT1	0.471	0.081	0.019
RT2	0.432	0.084	0.021
MT2	0.496	0.083	0.033
LT2	0.510	0.085	0.104
RT3	0.464	0.031	0.005
MT3	0.455	0.056	0.016
LT3	0.465	0.074	0.028
RT4	0.326	0.020	0.004
MT4	0.345	0.046	0.02
LT4	0.421	0.048	0.011
CBT4	0.408	0.053	0.027
RT5	0.160	0.012	0
MT5	0.164	0.006	0
LT5	0.215	0.020	0
OERS	0.347	0.018	0.032

associated microbial community (Dittmar and Lara 2001a). Mangrove forests can act as nitrogen sinks, especially in periods of increased plant growth with elevated air temperatures, increased solar radiation, or rainfall (Cunha et al. 2006, Bernini and Rezende 2010). During the dry season, with very high salinity values and little freshwater input through rainfall, plant growth, and litter production are likely reduced due to induced salinity and dryness stress (Mehlig 2001). This seemed to be reflected in the more conservative mixing of TDN concentrations in the dry season (Fig. 6), even so, we did not cover the lower to intermediate salinity ranges. In contrast, negative deviations of TDN concentrations compared to conservative mixing suggested that mangrove forests fringing the estuary acted as a sink during the rainy season. This suggests a pronounced seasonal dependency of N uptake in mangrove forests along the estuary (Fig. 6). The observed negative deviations of TDN concentrations from conservative mixing in the rainy season can be explained by an increased N uptake during periods of floral growth with elevated litter production (Wang et al. 2019) and peaking abundances of microphytobenthos (Benny et al. 2021). In the dry season, elevated salinity and dryness stress may cause reduced plant and microphytobenthos growth with lower nitrogen demand, resulting in more conservative TDN behavior.

Mangroves Change DOM Composition along an Estuarine Gradient.—To better understand DOM dynamics in the mangrove-fringed estuarine waters, we analyzed its molecular composition in relation to environmental parameters (Fig. 4).

Upstream samples were associated with elevated levels of polycyclic aromatic and highly aromatic compounds characterized by intensity-weighted average AI_{mod} values > 0.5 (groups 1 + 2; Fig. 4). These compounds are generally associated with terrestrial DOM originating from vascular plants containing higher portions of lignins, tannins, and their degradation products (Medeiros et al. 2015a, Seidel et al. 2015a). These compounds are also abundant in mangrove porewater DOM (Mori et al. 2019). Our data revealed a relative enrichment of compound groups 1 & 2 compared to

conservative mixing in the mangrove-fringed area in the dry season and rainy season (Figs. 6 and 7). These compounds can therefore be attributed to fluvial DOM with additional input from mangrove-derived DOM via porewater outwelling (Medeiros et al. 2015a, Seidel et al. 2015a, Mori et al. 2019) .

In the rainy season, samples from transects 2 and 3 were characterized by higher relative abundances of aromatic compounds (groups 1 and 2), values of intensity-weighted average AI_{mod}, and DBE indicating fresher and less degraded DOM mangrove and terrestrial systems (Fig. 4B; Mori et al. 2019). We assume that this was caused by DOM input from surface runoff during the rainy season introduced though the waters of a major tidal creek and of the da Dona River estuary entering the estuary just before these two transects. Both areas are dominated by thick mangrove forests with large tidal creeks, and geomorphological depressions. This explains the alterations in the biogeochemical parameters particularly at the left and middle positions of the transect 2 and the right position of transect 3 (Fig. 4B). However, the introduction of DOM was more pronounced at transect 2 compared to transect 3, as through the tidal creek surface runoff drains directly into the estuary along the transect without much time to mix with the estuarine waters causing notable changes of salinity and temperature (Fig. 3B and C). The runoff likely introduced fresher, less degraded terrestrial DOM from nearby mangrove forests, compared to more distant riverine stations upstream, where DOM travels longer distances before reaching the estuary. This may account for the additional input of fresher terrestrial DOM from the mangroves surrounding the Jaguaripe River estuary. Additionally, such flushing events have been shown in similar studies to increase sediment loads decreasing sunlight penetrating the water column (Medeiros and de Araújo 2013, Xu et al. 2021). Both, reduced resident times and decreased sunlight penetration depth, result in reduction of photochemical degradation (Rossel et al. 2013, Seidel et al. 2017) transforming aromatic DOM. Therefore, we assume that these runoffs directly into the estuary introduce fresher and less degraded DOM, i.e. from the mangroves in the area around the Jaguaripe River estuary.

Samples collected at locations further upstream, i.e., from transects 1 and 2, were characterized by high relative abundance of S-containing compounds (Fig. 4), and their relative abundances exceeded values expected from conservative mixing (Figs. 6 and 7). This indicated input from additional DOM sources along the transects in both, dry and rainy seasons. Similar trends have been observed in systems with prominent coastal vegetation, such as mangrove forests and salt marshes (Medeiros et al. 2015b, Mori et al. 2019, Knoke et al. 2024). These compounds likely originated from sulfidic mangrove-sediments where the abiotic incorporation of sulfide into DOM under sulfidic conditions leads to the formation of S-enriched DOM compounds (Seidel et al. 2014, Sleighter et al. 2014, Pohlabeln et al. 2017). Additionally, we found an increased input of saturated compounds with low O/C ratios along transects further away from the river mouth mainly in the dry season (group 5; Figs. 4A and 6). Patterns of increasing saturation levels can be linked to the increased utilization and reworking of DOM by microbes present in different aquatic environments (Seidel et al. 2015a, Osterholz et al. 2016). Microbial activity has been shown to cause a shift of DOM toward increased levels of saturated compounds with low O/C ratios (Kim et al. 2006, Seidel et al. 2014). An earlier study reported similar findings with an increased input of saturated, oxygen-poor compounds scattered along a mangrove-fringed estuary in tropical Australia (Mori et al. 2019). We conclude that the presence

of these compounds in the Jaguaripe River estuary is closely tied to the influx of porewater and surface runoff from nearby mangrove ecosystems. The reduced input of these compounds during the rainy season was likely due to dilution and the rapid transport of fluvial DOM through the estuary (Raymond et al. 2016, Letourneau and Medeiros 2019).

Our statistical analyses revealed that samples collected from transects closer to the coastal ocean exhibited increases in salinity, DO, and pH. During both seasons, these samples also had higher relative abundances of highly unsaturated DOM compounds, saturated compounds with high O/C ratios including carbohydrates, unsaturated aliphatics with and without nitrogen heteroatoms, as well as N and P-containing compounds (groups 3, 4, 6, 7; Tables 1 and 2, Figs. 4, 6, 7). These findings were consistent with previous studies that linked increasing salinity with higher proportions of saturated DOM, as well as increasing levels of N- and P-containing compounds (Seidel et al. 2015a, Osterholz et al. 2016, Seidel et al. 2017, He et al. 2020, Zhou et al. 2021). The increase in saturation levels is due to degradation and dilution of aromatic terrestrial with more aliphatic, marine DOM (Sleighter and Hatcher 2008, Seidel et al. 2015a, Osterholz et al. 2016, He et al. 2020). The increase in N- and P-containing DOM indicates an increased DOM input from autochthonous and marine sources linked to primary production (Sleighter and Hatcher 2008, Mori et al. 2019). However, our data also revealed the removal of N-containing and aliphatic DOM compounds along the transects in the rainy season (N and group 7; Fig. 7). We attribute this to the removal of TDN, as previously discussed. Nitrogen limitation in the system may cause microbial communities in mangrove sediments to utilize available nitrogen, including nitrogen-containing DOM, explaining its relative depletion during rainy season.

Additionally, P-containing compounds were removed in all transects as they traveled seaward during the rainy season (Fig. 7). A similar trend has been reported for a mangrove fringed estuary in a tropical region (Mori et al. 2019). The removal might be caused by the oligotrophy in the estuary and nearby Todos os Santos Bay resulting in an increased uptake by the mangrove associated microbial communities (Hatje et al. 2009, Reef et al. 2010, Ouyang and Guo 2016, Pan et al. 2017, Marins et al. 2020).

Tracing DOM Sources Based on Calculated Indices.—Analytical methods that have been used to trace terrestrial DOM at the land-ocean interface and in coastal waters commonly include measurements of $\delta^{13}C$ DOC and lignin composition (Mannino and Harvey 2000, Hernes and Benner 2003, Leigh McCallister et al. 2006). Molecular indexes, such as the I_{Terr} developed by Medeiros et al. (2016), using ultra-high resolution mass spectrometry data are becoming more widely used (Degenhardt et al. 2021, Waska et al. 2021, Maurischat et al. 2023), helping to better constrain the molecular DOM transformations from land to sea. As expected, in our data set, the I_{Terr} values decreased with increasing salinity (Figs. 2H and 3H), confirming its applicability to smaller tropical river systems, as it has been shown previously for subterranean and alpine river systems (Waska et al. 2021, Maurischat et al. 2023). In the rainy season, runoff from the mangrove creek north of transect 2 appeared to significantly impact estuarine waters, because elevated I_{Terr} values identified a clear input of terrigenous DOM in the left part of transect 2 (Fig. 3H). This area contains a large mangrove creek and, to some extent, Atlantic Forest vegetation, which probably

served as sources of terrestrial DOM. The I_{Terr} values indicated a dynamic shift of water exchange between the river and coastal ocean waters in the estuary. In the dry season, the seawater was pushed into the estuary along the left edge of the downstream transects, while riverine waters were pushed out on the right side of the river mouth (Fig. 2). In the rainy season, the I_{Terr} values indicated a stronger influx on the left side of the two downstream transects (Fig. 3H). This influx either originated from the terrestrial areas north of the connecting channel between the Jaguaripe River estuary and the Todos os Santos Bay, or from riverine input into the bay, that was transported through the connection directly into the estuary. The elevated I_{Terr} values on the left sides of transects 1 and 2 suggested increased terrigenous DOM input (Fig. 3H). This pattern likely resulted from surface runoff from the forests north of the estuary, which drains through tidal creeks in the mangrove zone into the estuary. The effect was especially pronounced in the left section of transect 2, where the largest tidal creeks probably contributed to the influx.

The I_{SuP} values displayed a very similar distribution pattern compared to the I_{Terr}. In the dry season, the seawater seemed to be pushed primarily into the left areas of the Jaguaripe River estuary (Fig. 2). The estuarine waters with high levels of DOM derived from the mangroves appeared to be flushed into the coastal waters on the right edge of the river mouth. The high I_{SuP} values in the upper river samples in both seasons could be caused by the excessive presence of the watergrass *Luziola spruceana* in the area. The watergrass extends along the edges of the upper Jaguaripe River, and its shallow riverbed just upstream of our upper river sampling site may serve as a source. Vegetated wetlands with waterlogged soils are known to export DOM in the form of CHOS compounds similar to mangrove forests (Lu et al. 2015, Gomez-Saez et al. 2017). A study in Delaware Bay found clusters of CHOS ($1 < H/C < 2$, $0.125 < O/C < 0.625$) likely originating from low salinity, potentially, sulfidic, saltmarshes (Powers et al. 2018). These molecular clusters aligned with three-quarters of the molecular formulae used for calculating the I_{SuP}. This suggests the need to cross-validate the applicability for this index, especially for systems heavily influenced by wetlands other than mangroves.

During the dry season, the highest values of I_{ManL} were found at sampling locations along transects 2 and 3 and in the outer estuary (Fig. 2). In these areas we observed local accumulations of minimally degraded floating mangrove leaf litter on the surface waters of the estuary. Our molecular analysis revealed that the leaf litter released substantial amounts of highly unsaturated DOM compounds (Fig. 6), including lignin degradation products and carboxyl-rich alicyclic molecules, confirming trends from previous studies (Brock et al. 2020, Hensgens et al. 2021). The elevated I_{ManL} value at the outer estuary likely corresponded to low tide sampling, when estuarine water flushed into the coastal zone, transporting fresh mangrove leaf litter and freshly leached leaf DOM.

Through tidal changes on average 1.05 (± 0.86) g of dry weight litter are being exported per m^2 mangrove forest per day (Golley et al. 1962, Lugo and Snedaker 1974, Woodroffe 1985a, b, Wattayakorn et al. 1990). Since only a small fraction of this leachate is transported into the coastal ocean within 24 hours (Camilleri and Ribi 1986, Tam et al. 1990, Chale 1993, Steinke et al. 1993, Davis and Childers 2007), developing an effective DOM tracing index was challenging. Additionally, fresh DOM is likely susceptible to rapid photo- and microbial-degradation (Rossel et al. 2013, Seidel et al. 2014, Seidel et al. 2015a), reducing the chance of detecting it. However,

we found low I_{ManL} values at the outer boundaries of the estuary (Tables 3 and 4, Fig. 4), suggesting that these compounds may impact microbial communities beyond the estuary, although the extent of this impact needs to be further quantified in future research. Interestingly, samples from the rainy season samples exhibited I_{ManL} values approximately an order of magnitude higher than those collected during the dry season (Tables 3 and 4), with particularly higher values at the left transect locations (Fig. 2J). We therefore assume, that these higher values were linked to increased surface runoffs from mangrove areas due to increased precipitation thus flushing more fresh leachate DOM into the estuary. As we did not include leaf leachates from terrestrial plants, there is also the possibility, that some of the compounds used to calculate the mangrove leaf leachate index could also be derived from leaf litter or organic matter deposits of other vascular plants. The DOM flushed into the estuarine waters, therefore, may not have been exclusively mangrove-derived, but also from terrestrial vegetation such as remains of the tropical Atlantic Forest in the area. The highly unsaturated compounds used for our index calculations are known to originate from such terrestrial sources (Seidel et al. 2014, Seidel et al. 2015a, Brock et al. 2020, Hensgens et al. 2021). However, we tried to limit the influence of nonmangrove terrestrial DOM compounds on the I_{ManL} by subtracting all compounds found in upstream river samples. Nevertheless, further testing of the I_{ManL} with a broader variety of leaf leachate samples is essential for the verification and potential improvement of the index in future studies. Initial steps should include confirming the effective tracing capacity of the I_{ManL} in other estuarine systems and testing unique biomarkers against DOM leached from other mangrove and terrestrial plant leaves to refine the index.

Conclusions

By combining the analysis of environmental parameters with nontargeted molecular DOM analysis we identified the biogeochemical dynamics of DOM driven by the mangrove forests fringing the Jaguaripe River estuary. Especially in the dry season, mangroves were a source for DOM thereby shaping the DOM composition in the estuary. This effect was particularly strong near mangrove forests rivaling the influence of other terrestrial DOM sources. However, in the rainy season, the input of DOM was less pronounced probably due to the increased freshwater input from precipitation and runoff flushing the estuary. The mangroves acted as a sink for TDN and N-containing aliphatics in the rainy season, likely because their increased N demand reduced its availability in the system. Our results support previous studies indicating that mangroves can act simultaneously as both sources and sinks for different DOM groups. Using a novel mangrove index we were able to trace DOM leached from mangrove leaves directly into the estuarine waters and even detected this fresh, potentially bioavailable, DOM beyond the estuary. However, while this is a promising approach, the I_{ManL} index requires further validation and potential adjustments to ensure its broader applicability as a robust tool for tracing mangrove-derived DOM in different systems.

Acknowledgments

We acknowledge the Leibniz Institute for Marine Research (ZMT) and the German Academic Exchange Service (DAAD) for providing funds (Grant number 57438025). MS and TD acknowledge funding by the Cluster of Excellence EXC 2077 (Project number 390741603). We thank all the volunteers and colleagues from the Centro Interdisciplinar de Energia e Ambiente (CIEnAm) and ZMT who helped with the sample collection and processing, especially M Zimmer, GMO Abuchahla, and M Santos-Andrade. We thank our colleagues at the Institute for Chemistry and Biology of the Marine Environment (ICBM) for their technical assistance during the analyses of the samples, especially K Klaproth and M Knoke. We thank the editor and two anonymous reviewers for their time and thoughtful comments which greatly improved the clarity of a previous manuscript version.

Literature Cited

Aguiar AL, Valle-Levinson A, Cirano M, Marta-Almeida M, Lessa GC, Paniagua-Arroyave JF. 2019. Ocean-estuary exchange variability in a large tropical estuary. Cont Shelf Res. 172:33–49. https://doi.org/10.1016/j.csr.2018.11.001

Bauer JE, Bianchi TS. 2011. Dissolved organic carbon cycling and transformation. *In:* Wolanski E, McLusky DE, editors. Treatise on estuarine and coastal science. Waltham: Academic Press. Vol 5. p. 7–67.

Benny N, Thomas LC, Padmakumar KB. 2021. Community structure of microphytobenthos associated with mangrove ecosystems along the southwest coast of India. Estuaries Coasts. 44(5):1380–1391. https://doi.org/10.1007/s12237-020-00888-w

Bernini E, Rezende CE. 2010. Litterfall in a mangrove in Southeast Brazil. Pan-Am J Aquat Sci. 5(4):508–519.

Boto KG, Bunt JS. 1981. Tidal export of particulate organic matter from a Northern Australian mangrove system. Estuar Coast Shelf Sci. 13(3):247–255. https://doi.org/10.1016/S0302-3524(81)80023-0

Bouillon S, Borges AV, Castañeda-Moya E, Diele K, Dittmar T, Duke NC, Kristensen E, Lee SY, Marchand C, Middelburg JJ, et al. 2008. Mangrove production and carbon sinks: a revision of global budget estimates. Global Biogeochem Cycles. 22(2):GB2013. https://doi.org/10.1029/2007GB003052

Brock O, Helmus R, Kalbitz K, Jansen B. 2020. Non-target screening of leaf litter-derived dissolved organic matter using liquid chromatography coupled to high-resolution mass spectrometry (LC-QTOF-MS). Eur J Soil Sci. 71(3):420–432. https://doi.org/10.1111/ejss.12894

Bunting P, Rosenqvist A, Hilarides L, Lucas RM, Thomas N, Tadono T, Worthington TA, Spalding M, Murray NJ, Rebelo L-M. 2022. Global mangrove extent change 1996–2020: Global Mangrove Watch Version 3.0. Remote Sens. 14(15):3657. https://doi.org/10.3390/rs14153657

Camilleri JC, Ribi G. 1986. Leaching of dissolved organic carbon (DOC) from dead leaves, formation of flakes from DOC, and feeding on flakes by crustaceans in mangroves. Mar Biol. 91(3):337–344. https://doi.org/10.1007/BF00428627

Chale FMM. 1993. Degradation of mangrove leaf litter under aerobic conditions. Hydrobiologia. 257(3):177–183. https://doi.org/10.1007/BF00765010

Cunha SR, Tognella-de-Rosa MMP, Costa CSB. 2006. Structure and litter production of mangrove forests under different tidal influences. J Coast Res. II(39):1169–1174.

Davis SE, Childers DL. 2007. Importance of water source in controlling leaf leaching losses in a dwarf red mangrove (*Rhizophora mangle* L.) wetland. Estuar Coast Shelf Sci. 71(1–2):194–201. https://doi.org/10.1016/j.ecss.2006.07.010

Degenhardt J, Merder J, Heyerhoff B, Simon H, Engelen B, Waska H. 2021. Cross-shore and depth zonations in bacterial diversity are linked to age and source of dissolved organic

matter across the intertidal area of a sandy beach. Microorganisms. 9(8):1720. https://doi.org/10.3390/microorganisms9081720
Dittmar T, Hertkorn N, Kattner G, Lara RJ. 2006. Mangroves, a major source of dissolved organic carbon to the oceans. Global Biogeochem Cycles. 20(1):2005GB002570. https://doi.org/10.1029/2005GB002570
Dittmar T, Koch B, Hertkorn N, Kattner G. 2008. A simple and efficient method for the solid-phase extraction of dissolved organic matter (SPE-DOM) from seawater. Limnol Oceanogr Methods. 6(6):230–235. https://doi.org/10.4319/lom.2008.6.230
Dittmar T, Lara RJ. 2001a. Driving forces behind nutrient and organic matter dynamics in a mangrove tidal creek in North Brazil. Estuar Coast Shelf Sci. 52(2):249–259. https://doi.org/10.1006/ecss.2000.0743
Dittmar T, Lara RJ. 2001b. Do mangroves rather than rivers provide nutrients to coastal environments south of the Amazon River? Evidence from long-term flux measurements. Mar Ecol Prog Ser. 213:67–77. https://doi.org/10.3354/meps213067
Dittmar T, Lara RJ, Kattner G. 2001. River or mangrove? Tracing major organic matter sources in tropical Brazilian coastal waters. Mar Chem. 73(3–4):253–271. https://doi.org/10.1016/S0304-4203(00)00110-9
Fechine GJM, Rabello MS, Souto Maior RM, Catalani LH. 2004. Surface characterization of photodegraded poly(ethylene terephthalate). The effect of ultraviolet absorbers. Polymer (Guildf). 45(7):2303–2308. https://doi.org/10.1016/j.polymer.2004.02.003
Golley F, Odum HT, Wilson RF. 1962. The structure and metabolism of a Puerto Rican red mangrove forest in May. Ecology. 43(1):9–19. https://doi.org/10.2307/1932034
Gomez-Saez GV, Pohlabeln AM, Stubbins A, Marsay CM, Dittmar T. 2017. Photochemical alteration of dissolved organic sulfur from sulfidic porewater. Environ Sci Technol. 51(24):14144–14154. https://doi.org/10.1021/acs.est.7b03713
Green NW, Perdue EM, Aiken GR, Butler KD, Chen H, Dittmar T, Niggemann J, Stubbins A. 2014. An intercomparison of three methods for the large-scale isolation of oceanic dissolved organic matter. Mar Chem, 161:14–19. https://doi.org/10.1016/j.marchem.2014.01.12
Hatje V, Barros F. 2012. Overview of the 20th century impact of trace metal contamination in the estuaries of Todos os Santos Bay: past, present and future scenarios. Mar Pollut Bull. 64(11):2603–2614. https://doi.org/10.1016/j.marpolbul.2012.07.009
Hatje V, de Andrade JB, Caroso C, Tavares F, Pereira CL. Bahia (Brazil : State), Fundação de Amparo à Pesquisa do Estado da Bahia, editors. 2009. Baía de Todos os Santos. Salvador, Bahia: EDUFBA.
Hatje V, Macedo SM, de Jesus RM, Cotrim G, Garcia KS, de Queiroz AF, Ferreira SLC. 2010. Inorganic as speciation and bioavailability in estuarine sediments of Todos os Santos Bay, BA, Brazil. Mar Pollut Bull. 60(12):2225–2232. https://doi.org/10.1016/j.marpolbul.2010.08.014
Hatje V, Masqué P, Patire VF, Dórea A, Barros F. 2021. Blue carbon stocks, accumulation rates, and associated spatial variability in Brazilian mangroves. Limnol Oceanogr. 66(2):321–334. https://doi.org/10.1002/lno.11607
He C, Pan Q, Li P, Xie W, He D, Zhang C, Shi Q. 2020. Molecular composition and spatial distribution of dissolved organic matter (DOM) in the Pearl River Estuary, China. Environ Chem. 17(3):240. https://doi.org/10.1071/EN19051
Hensgens G, Lechtenfeld OJ, Guillemette F, Laudon H, Berggren M. 2021. Impacts of litter decay on organic leachate composition and reactivity. Biogeochemistry. 154(1):99–117. https://doi.org/10.1007/s10533-021-00799-3
Hernes PJ, Benner R. 2003. Photochemical and microbial degradation of dissolved lignin phenols: implications for the fate of terrigenous dissolved organic matter in marine environments. J Geophys Res Oceans. 108(C9):2002JC001421. https://doi.org/10.1029/2002JC001421
Hertkorn N, Harir M, Cawley KM, Schmitt-Kopplin P, Jaffé R. 2016. Molecular characterization of dissolved organic matter from subtropical wetlands: a comparative study through the analysis of optical properties, NMR and FTICR/MS. Biogeosciences, 13(8):2257–2277. https://doi.org/10.5194/bg-13-2257-2016

INMET. 2019. Dados de precipitação na estação "Radio Farol, Salvador, Bahia" 2008–2018. Available from: https://portal.inmet.gov.br/

Kim S, Kaplan LA, Hatcher PG. 2006. Biodegradable dissolved organic matter in a temperate and a tropical stream determined from ultra-high resolution mass spectrometry. Limnol Oceanogr. 51(2):1054–1063. https://doi.org/10.4319/lo.2006.51.2.1054

Knoke M, Dittmar T, Zielinski O, Kida M, Asp NE, De Rezende CE, Schnetger B, Seidel M. 2024. Outwelling of reduced porewater drives the biogeochemistry of dissolved organic matter and trace metals in a major mangrove-fringed estuary in Amazonia. Limnol Oceanogr. 69(2):262–278. https://doi.org/10.1002/lno.12473

Koch BP, Dittmar T. 2006. From mass to structure: an aromaticity index for high-resolution mass data of natural organic matter. Rapid Commun Mass Spectrom. 20(5):926–932. https://doi.org/10.1002/rcm.2386

Koch BP, Dittmar T. 2016. Erratum: From mass to structure: an aromaticity index for high-resolution mass data of natural organic matter Rapid Commun Mass Spectrom. 30(1):250. https://doi.org/10.1002/rcm.7433

Kristensen E, Bouillon S, Dittmar T, Marchand C. 2008. Organic carbon dynamics in mangrove ecosystems: a review. Aquat Bot. 89(2):201–219. https://doi.org/10.1016/j.aquabot.2007.12.005

Krull M, Abessa DMS, Hatje V, Barros F. 2014. Integrated assessment of metal contamination in sediments from two tropical estuaries. Ecotoxicol Environ Saf. 106:195–203. https://doi.org/10.1016/j.ecoenv.2014.04.038

Kusel K, Drake HL. 1996. Anaerobic capacities of leaf litter. Appl Environ Microbiol. 62(11):4216–4219. https://doi.org/10.1128/aem.62.11.4216-4219.1996

Leigh McCallister S, Bauer JE, Canuel EA. 2006. Bioreactivity of estuarine dissolved organic matter: a combined geochemical and microbiological approach. Limnol Oceanogr. 51(1):94–100. https://doi.org/10.4319/lo.2006.51.1.0094

Letourneau ML, Medeiros PM. 2019. Dissolved organic matter composition in a marsh-dominated estuary: response to seasonal forcing and to the passage of a hurricane. J Geophys Res Biogeosci. 124(6):1545–1559. https://doi.org/10.1029/2018JG004982

Lu Y, Li X, Mesfioui R, Bauer JE, Chambers RM, Canuel EA, Hatcher PG. 2015. Use of ESI-FTICR-ms to characterize dissolved organic matter in headwater streams draining forest-dominated and pasture-dominated watersheds. PLOS ONE. 10(12):e0145639. https://doi.org/10.1371/journal.pone.0145639

Lugo AE, Snedaker SC. 1974. The ecology of mangroves. Annu Rev Ecol Syst. 5(1):39–64. https://doi.org/10.1146/annurev.es.05.110174.000351

Maher DT, Santos IR, Golsby-Smith L, Gleeson J, Eyre BD. 2013. Groundwater-derived dissolved inorganic and organic carbon exports from a mangrove tidal creek: the missing mangrove carbon sink? Limnol Oceanogr. 58(2):475–488. https://doi.org/10.4319/lo.2013.58.2.0475

Mannino A, Harvey HR. 2000. Terrigenous dissolved organic matter along an estuarine gradient and its flux to the coastal ocean. Org Geochem. 31(12):1611–1625. https://doi.org/10.1016/S0146-6380(00)00099-1

Marins RV, Lacerda LD, Araújo ICS, Fonseca LV, Silva FATF. 2020. Phosphorus and suspended matter retention in mangroves affected by shrimp farm effluents in NE Brazil. An Acad Bras Cienc. 92(3):e20200758. https://doi.org/10.1590/0001-3765202020200758

Maurischat P, Seidel M, Dittmar T, Guggenberger G. 2023. Complex dissolved organic matter (DOM) on the roof of the world – Tibetan DOM molecular characteristics indicate sources, land use effects, and processing along the fluvial–limnic continuum. Biogeosciences. 20(14):3011–3026. https://doi.org/10.5194/bg-20-3011-2023

Medeiros PHA, de Araújo JC. 2013. Temporal variability of rainfall in a semiarid environment in Brazil and its effect on sediment transport processes. J Soils Sediments. 14:1216–1223. https://doi.org/10.1007/s11368-013-0809-9

Medeiros PM, Seidel M, Dittmar T, Whitman WB, Moran MA. 2015b. Drought-induced variability in dissolved organic matter composition in a marsh-dominated estuary. Geophys Res Lett. 42(15):6446–6453. https://doi.org/10.1002/2015GL064653

Medeiros PM, Seidel M, Niggemann J, Spencer RGM, Hernes PJ, Yager PL, Miller WL, Dittmar T, Hansell DA. 2016. A novel molecular approach for tracing terrigenous dissolved organic matter into the deep ocean. Global Biogeochem Cycles. 30(5):689–699. https://doi.org/10.1002/2015GB005320

Medeiros PM, Seidel M, Ward ND, Carpenter EJ, Gomes HR, Niggemann J, Krusche AV, Richey JE, Yager PL, Dittmar T. 2015a. Fate of the Amazon River dissolved organic matter in the tropical Atlantic Ocean. Global Biogeochem Cycles. 29(5):677–690. https://doi.org/10.1002/2015GB005115

Mehlig U. 2001. Aspects of tree primary production in an equatorial mangrove forest in Brazil. PhD Dissertation. Cent Trop Mar Ecol ZMT Contrib No 14:155.

Merder J, Freund JA, Feudel U, Hansen CT, Hawkes JA, Jacob B, Klaproth K, Niggemann J, Noriega-Ortega BE, Osterholz H, et al. 2020. ICBM-OCEAN: processing ultra-high resolution mass spectrometry data of complex molecular mixtures. Anal Chem. 92(10):6832–6838. https://doi.org/10.1021/acs.analchem.9b05659

Mori C, Santos IR, Brumsack HJ, Schnetger B, Dittmar T, Seidel M. 2019. Non-conservative behavior of dissolved organic matter and trace metals (Mn, Fe, Ba) driven by porewater exchange in a subtropical mangrove-estuary. Front Mar Sci. 6:481. https://doi.org/10.3389/fmars.2019.00481

Oksanen J, Blanchet FG, Friendly M, Kindt R, Legendre P, Mcglinn D, Minchin PR, O'Hara RB, Simpson GL, Solymos P, et al. 2020. vegan: community ecology package. R Package v25-7. Available from: https://cran.r-project.org/package=vegan

Osterholz H, Kirchman DL, Niggemann J, Dittmar T. 2016. Environmental drivers of dissolved organic matter molecular composition in the Delaware estuary. Front Earth Sci. 4:95. https://doi.org/10.3389/feart.2016.00095

Ouyang X, Guo F. 2016. Paradigms of mangroves in treatment of anthropogenic wastewater pollution. Sci Total Environ. 544:971–979. https://doi.org/10.1016/j.scitotenv.2015.12.013

Oyane A, Sakamaki I, Pyatenko A, Nakamura M, Ishikawa Y, Shimizu Y, Kawaguchi K, Koshizaki N. 2014. Laser-assisted calcium phosphate deposition on polymer substrates in supersaturated solutions. RSC Advances. 4(96):53645–53648. https://doi.org/10.1039/C4RA09313E

Palit K, Rath S, Chatterjee S, Das S. 2022. Microbial diversity and ecological interactions of microorganisms in the mangrove ecosystem: threats, vulnerability, and adaptations. Environ Sci Pollut Res Int. 29(22):32467–32512. https://doi.org/10.1007/s11356-022-19048-7

Pan F, Liu H, Guo Z, Li Z, Wang B, Gao A. 2017. Geochemical behavior of phosphorus and iron in porewater in a mangrove tidal flat and associated phosphorus input into the ocean. Cont Shelf Res. 150:65–75. https://doi.org/10.1016/j.csr.2017.09.012

Pohlabeln AM, Gomez-Saez GV, Noriega-Ortega BE, Dittmar T. 2017. Experimental evidence for abiotic sulfurization of marine dissolved organic matter. Front Mar Sci. 4:364. https://doi.org/10.3389/fmars.2017.00364

Powers LC, Luek JL, Schmitt-Kopplin P, Campbell BJ, Magen C, Cooper LW, Gonsior M. 2018. Seasonal changes in dissolved organic matter composition in Delaware Bay, USA in March and August 2014. Org Geochem. 122:87–97. https://doi.org/10.1016/j.orggeochem.2018.05.005

R Core Team. 2019. R: a language and environment for statistical computing. Vienna, Austria: R Foundation for Statistical Computing. Available from: https://www.R-project.org/

Ray R, Baum A, Rixen T, Gleixner G, Jana TK. 2018. Exportation of dissolved (inorganic and organic) and particulate carbon from mangroves and its implication to the carbon budget in the Indian Sundarbans. Sci Total Environ. 621:535–547. https://doi.org/10.1016/j.scitotenv.2017.11.225

Raymond PA, Saiers JE, Sobczak WV. 2016. Hydrological and biogeochemical controls on watershed dissolved organic matter transport: pulse- shunt concept. Ecology. 97(1):5–16. https://doi.org/10.1890/14-1684.1

Reef R, Feller IC, Lovelock CE. 2010. Nutrition of mangroves. Tree Physiol. 30(9):1148–1160. https://doi.org/10.1093/treephys/tpq048

Reis CRG, Nardoto GB, Oliveira RS. 2017. Global overview on nitrogen dynamics in mangroves and consequences of increasing nitrogen availability for these systems. Plant Soil. 410(1–2):1–19. https://doi.org/10.1007/s11104-016-3123-7

Reith F, Drake HL, Küsel K. 2002. Anaerobic activities of bacteria and fungi in moderately acidic conifer and deciduous leaf litter. FEMS Microbiol Ecol. 41(1):27–35. https://doi.org/10.1111/j.1574-6941.2002.tb00963.x

Riedel T, Dittmar T. 2014. A method detection limit for the analysis of natural organic matter via Fourier transform ion cyclotron resonance mass spectrometry. Anal Chem. 86(16):8376–8382. https://doi.org/10.1021/ac501946m

Rossel PE, Vähätalo AV, Witt M, Dittmar T. 2013. Molecular composition of dissolved organic matter from a wetland plant (*Juncus effusus*) after photochemical and microbial decomposition (1.25 yr): common features with deep sea dissolved organic matter. Org Geochem. 60:62–71. https://doi.org/10.1016/j.orggeochem.2013.04.013

Santos IR, Burnett WC, Dittmar T, Suryaputra IGNA, Chanton J. 2009. Tidal pumping drives nutrient and dissolved organic matter dynamics in a Gulf of Mexico subterranean estuary. Geochim Cosmochim Acta. 73(5):1325–1339. https://doi.org/10.1016/j.gca.2008.11.029

Seidel M, Beck M, Greskowiak J, Riedel T, Waska H, Suryaputra IGNA, Schnetger B, Niggemann J, Simon M, Dittmar T. 2015b. Benthic-pelagic coupling of nutrients and dissolved organic matter composition in an intertidal sandy beach. Mar Chem. 176:150–163. https://doi.org/10.1016/j.marchem.2015.08.011

Seidel M, Beck M, Riedel T, Waska H, Suryaputra IGNA, Schnetger B, Niggemann J, Simon M, Dittmar T. 2014. Biogeochemistry of dissolved organic matter in an anoxic intertidal creek bank. Geochim Cosmochim Acta. 140:418–434. https://doi.org/10.1016/j.gca.2014.05.038

Seidel M, Manecki M, Herlemann DPR, Deutsch B, Schulz-Bull D, Jürgens K, Dittmar T. 2017. Composition and transformation of dissolved organic matter in the Baltic Sea. Front Earth Sci. 5:31. https://doi.org/10.3389/feart.2017.00031

Seidel M, Yager PL, Ward ND, Carpenter EJ, Gomes HR, Krusche AV, Richey JE, Dittmar T, Medeiros PM. 2015a. Molecular-level changes of dissolved organic matter along the Amazon River-to-ocean continuum. Mar Chem. 177(2):218–231. https://doi.org/10.1016/j.marchem.2015.06.019

Sleighter RL, Chin YP, Arnold WA, Hatcher PG, McCabe AJ, McAdams BC, Wallace GC. 2014. Evidence of incorporation of abiotic S and N into prairie wetland dissolved organic matter. Environ Sci Technol Lett. 1(9):345–350. https://doi.org/10.1021/ez500229b

Sleighter RL, Hatcher PG. 2008. Molecular characterization of dissolved organic matter (DOM) along a river to ocean transect of the lower Chesapeake Bay by ultra-high resolution electrospray ionization Fourier transform ion cyclotron resonance mass spectrometry. Mar Chem. 110(3–4):140–152. https://doi.org/10.1016/j.marchem.2008.04.008

Spalding M, Kainuma M, Collins L. 2010. World atlas of mangroves. 1st ed. London: Routledge.

Steinke TD, Holland AJ, Singh Y. 1993. Leaching losses during decomposition of mangrove leaf litter. S Afr J Bot. 59(1):21–25. https://doi.org/10.1016/S0254-6299(16)30770-0

Stenson AC, Marshall AG, Cooper WT. 2003. Exact masses and chemical formulas of individual Suwannee River fulvic acids from ultra-high resolution electrospray ionization fourier transform ion cyclotron resonance mass spectra. Anal Chem. 75(6):1275–1284. https://doi.org/10.1021/ac026106p

Tam NFY, Vrijmoed LLP, Wong YS. 1990. Nutrient dynamics associated with leaf decomposition in a small subtropical mangrove community in Hong Kong. Bull Mar Sci. 47:68–78.

Thomson T, Fusi M, Bennett-Smith MF, Prinz N, Aylagas E, Carvalho S, Lovelock CE, Jones BH, Ellis JI. 2022. Contrasting effects of local environmental and biogeographic factors on

the composition and structure of bacterial communities in arid monospecific mangrove soils. Microbiol Spectr. 10(1):e00903-21. https://doi.org/10.1128/spectrum.00903-21

Wang F, Chen N, Yan J, Lin J, Guo W, Cheng P, Liu Q, Huang B, Tian Y. 2019. Major processes shaping mangroves as inorganic nitrogen sources or sinks: insights from a multidisciplinary study. J Geophys Res Biogeosci. 124(5):1194–1208. https://doi.org/10.1029/2018JG004875

Waska H, Simon H, Ahmerkamp S, Greskowiak J, Ahrens J, Seibert SL, Schwalfenberg K, Zielinski O, Dittmar T. 2021. Molecular traits of dissolved organic matter in the subterranean estuary of a high-energy beach: indications of sources and sinks. Front Mar Sci. 8:607083. https://doi.org/10.3389/fmars.2021.607083

Wattayakorn G, Wolanski E, Kjerfve B. 1990. Mixing, trapping and outwelling in the Klong Ngao mangrove swamp, Thailand. Estuar Coast Shelf Sci. 31(5):667–688. https://doi.org/10.1016/0272-7714(90)90019-N

Woodroffe CD. 1985a. Studies of a mangrove basin, Tuff Crater, New Zealand: III. The flux of organic and inorganic particulate matter. Estuar Coast Shelf Sci. 20(4):447–461. https://doi.org/10.1016/0272-7714(85)90088-5

Woodroffe CD. 1985b. Studies of a mangrove basin, Tuff Crater, New Zealand: I. Mangrove biomass and production of detritus. Estuar Coast Shelf Sci. 20(3):265–280. https://doi.org/10.1016/0272-7714(85)90042-3

Xu Z, Zhang S, Yang X. 2021. Water and sediment yield response to extreme rainfall events in a complex large river basin: a case study of the Yellow River Basin, China. J Hydrol (Amst). 597:126183. https://doi.org/10.1016/j.jhydrol.2021.126183

Zark M, Christoffers J, Dittmar T. 2017. Molecular properties of deep-sea dissolved organic matter are predictable by the central limit theorem: evidence from tandem FT-ICR-MS. Mar Chem. 191:9–15. https://doi.org/10.1016/j.marchem.2017.02.005

Zhou Y, He D, He C, Li P, Fan D, Wang A, Zhang K, Chen B, Zhao C, Wang Y, et al. 2021. Spatial changes in molecular composition of dissolved organic matter in the Yangtze River Estuary: implications for the seaward transport of estuarine DOM. Sci Total Environ. 759:143531. https://doi.org/10.1016/j.scitotenv.2020.143531